Geological Society of America
Field Guide 6
2005

Neotectonics and paleoseismology of the Wasatch fault, Utah

Ronald L. Bruhn*
Department of Geology and Geophysics, University of Utah, Salt Lake City, Utah 84112, USA

Christopher B. DuRoss*
Utah Geological Survey, 1594 West North Temple, #3110, Salt Lake City, Utah 84116, USA

Ronald A. Harris*
Department of Geology, Brigham Young University, Provo, Utah 84602, USA

William R. Lund*
Utah Geological Survey, Southern Utah Regional Office, 88 East Fiddler Canyon Road, Cedar City, Utah 84720, USA

ABSTRACT

The Wasatch fault is a 370-km-long zone of normal faulting that forms the eastern edge of the Basin and Range Province in Utah and southeastern Idaho. The fault zone is subdivided into ten segments that range from 30 to 60 km in length and are each capable of generating earthquakes of M ~7. For the five central segments, multiple surface-faulting earthquakes have occurred during the Holocene, and vertical slip rates are ~1 mm/yr. Recurrence intervals for the individual central segments range from ~1300 to 2500 yr. The fault poses a significant seismic hazard to the highly urbanized Wasatch Front in north-central Utah. The field localities described in this guide provide an overview of the surface and subsurface character of the Wasatch fault zone. Five field trip stops are located along the Nephi, Provo, and Salt Lake City segments. We will observe fault scarps on Quaternary deposits, which record tectonic displacements associated with Holocene earthquakes, and fault-zone rocks exhumed from depths in excess of 10 km that are hydrothermally altered and have evidence of brittle and ductile deformation. Specific topics of discussion include the nature of piedmont fault scarps; the use of paleoseismic trenching and fault-scarp geomorphology to infer earthquake timing, recurrence intervals, and fault slip rates; and the subsurface structure and rheology of the fault.

Keywords: faulting, paleoseismology, neotectonics, earthquake geology.

INTRODUCTION

The Wasatch normal fault is one of the preeminent tectonic structures of North America. The fault has a profound physiographic expression on the landscape of the western United States and poses a significant earthquake hazard to the densely populated urban corridor of north-central Utah. The Wasatch fault played a central role in the evolution of geological thought in the latter nineteenth and early twentieth centuries, when geologists began pondering the landscape and geological structure of the Great Basin (Emmons, 1878; King, 1878; Gilbert, 1884, 1928;

*E-mails bruhn@earth.utah.edu; christopherduross@utah.gov; ron_harris@byu.edu; billlund@utah.gov.

Bruhn, R.L., DuRoss, C.B., Harris, R.A., and Lund, W.R., 2005, Neotectonics and paleoseismology of the Wasatch fault, Utah, *in* Pederson, J., and Dehler, C.M., eds., Interior Western United States: Geological Society of America Field Guide 6, p. 231–250, doi: 10.1130/2005.fld006(11). For permission to copy, contact editing@geosociety.org. © 2005 Geological Society of America

Pack, 1926). Subsequently, the Wasatch fault regained prominence in the latter part of the twentieth century when it played a significant role in the development of modern paleoseismology. Studies of the Wasatch fault contributed directly to the concept of "characteristic" earthquakes (Schwartz and Coppersmith, 1984) and to our understanding of colluvial-wedge formation, the recurrence patterns of normal faulting (e.g., Machette et al., 1992; McCalpin, 1996; Lund, 2005), and the mechanics of earthquake generation (Parry and Bruhn, 1986; Bruhn et al., 1990, 1994). Today, the fault remains an important natural laboratory for investigating the structure, tectonic geomorphology, earthquake-recurrence patterns, and rupture segmentation of active normal faults. Considerable effort is currently directed at reconciling differences in slip rates inferred from Quaternary geology versus geodetic measurements, a topic of fundamental importance to tectonophysics as well as the field of earthquake hazards (Chang and Smith, 2002; Friedrich et al., 2003).

The topographic escarpment of the Wasatch Range rises abruptly along the eastern side of the Wasatch fault (Fig. 1), forming the physiographic boundary between the Rocky Mountains or the Colorado Plateau and the Basin and Range Province to the west. Evidence for active faulting is both abundant and well displayed where piedmont fault scarps cross Quaternary alluvial fans (Fig. 2), glacial moraines, and deltas and shorelines of Pleistocene Lake Bonneville. Paleoseismic trenching of these faulted deposits reveals a rich and varied history of late Pleistocene and Holocene earthquakes, providing a tantalizing glimpse into temporal patterns of earthquake recurrence—the "pulse" of the earthquake engine. The geomorphology and structure of the Wasatch mountain front also contain clues as to the geometry, composition, and mechanical characteristics of the fault at depth. When taken collectively, this information allows us to peer into the heart of the earthquake engine itself.

During our field trip, we will visit localities along three of the ten proposed rupture segments of the Wasatch fault (Fig. 1). The goal is to observe and discuss the fault from the surface to depths in excess of 10 km, where M 7 earthquakes presumably originate. We will observe and discuss aspects of the tectonic geomorphology and Quaternary geology, as well as visit a paleoseismic trench excavation and localities where deformed rocks are exhumed from deep within the fault zone. Specific topics considered include the nature of piedmont fault scarps, the use of paleoseismic trenching and geomorphology surveys to infer fault-rupture parameters (e.g., earthquake timing, recurrence, and displacement), and the structure and rheology of the fault in the subsurface.

WASATCH FAULT—TECTONICS AND STRUCTURE

The Wasatch normal fault extends for ~370 km from southern Idaho into central Utah, passing directly through the densely populated and rapidly expanding urban corridor along the front of the Wasatch Range. The fault is subdivided into ten segments that vary from roughly 30–60 km in length and that were originally thought to be independent rupture segments based on differences in Holocene earthquake histories (Schwartz and Coppersmith, 1984). This concept is currently being challenged as more information on earthquake timing is obtained and the implications of event-dating uncertainties are further explored (Chang and Smith, 2002; DuRoss and Bruhn, 2005; Lund, 2005). The segment boundaries are also interesting from a structural perspective because they are marked by bedrock spurs that extend into adjacent basins, by changes in the topography along the Wasatch Range crest, and by jogs and bends in the fault trace (Gilbert, 1928; Schwartz and Coppersmith, 1984; Bruhn et al., 1992; Wheeler and Krystinik, 1992). Each segment is capable of generating earthquakes of M ~7. Although no such earthquakes have occurred in historical time, the six central segments (Brigham City to Levan segments; Fig. 1) have ruptured in large magnitude earthquakes that created surface displacement during the Holocene. Recurrence intervals of surface-faulting earthquakes vary from segment to segment, but for the five central segments (not including the Levan segment) average roughly 1300 yr to 2500 yr in each segment, or about once every three to five hundred years when considered collectively (Machette et al., 1992; McCalpin and Nishenko, 1996; Lund, 2005). Surface displacement or net vertical tectonic displacement (Swan et al., 1980) averages ~2 m during surface-faulting earthquakes, but varies along the length of the rupture.

Structurally, the Wasatch fault is an aggregate of normal faults that nucleated, grew in length, and linked together to form a continuous normal fault zone. The process of growth and linkage is reflected in the geometry of the ten fault segments (Wheeler and Krystinik, 1992), variations in the amount of cumulative displacement along strike, differences in the amount of flexure and rotation of the footwall, and the structure of hanging wall basins (e.g., Zoback, 1983; Mabey, 1992; Armstrong et al., 2003, 2004). The initiation of faulting is partly constrained by radiometric dating of fault rock (Parry et al., 1988), by the onset of Neogene sedimentation in the eastern Great Basin (Bryant et al., 1989), and by the thermochronology of the Wasatch Range (e.g., Evans et al., 1985; Kowallis et al., 1990). The central part of the Wasatch fault may have formed as early as 17.6 ± 0.7 Ma based on a K-Ar age of sericite obtained from the fault zone near Salt Lake City, where deformed rocks were exhumed from a depth of ~11 km (Parry and Bruhn, 1987). By 10–12 Ma, faulting was clearly under way, based on an influx of sedimentary detritus into basins west of the Wasatch Range and the fission track thermochronology of the Wasatch Range (Armstrong et al., 2003, 2004). Vertical slip rates averaged over the past 10 Ma vary from 0.4 to 0.7 mm/yr, somewhat lower than the 1 mm/yr average obtained from fault trench studies (Machette et al., 1992; Friedrich et al., 2003; Lund, 2005). The contemporary rate of horizontal extension measured by geodetic surveying (using GPS networks) is 2.7 ± 1.3 mm/yr in the central part of the fault zone (Martinez et al., 1998). If accounted for by seismic processes, the Wasatch fault geodetic rate would suggest a higher frequency of large ($M \geq 6.6$) earthquakes than supported by paleoseismic and historical-seismicity

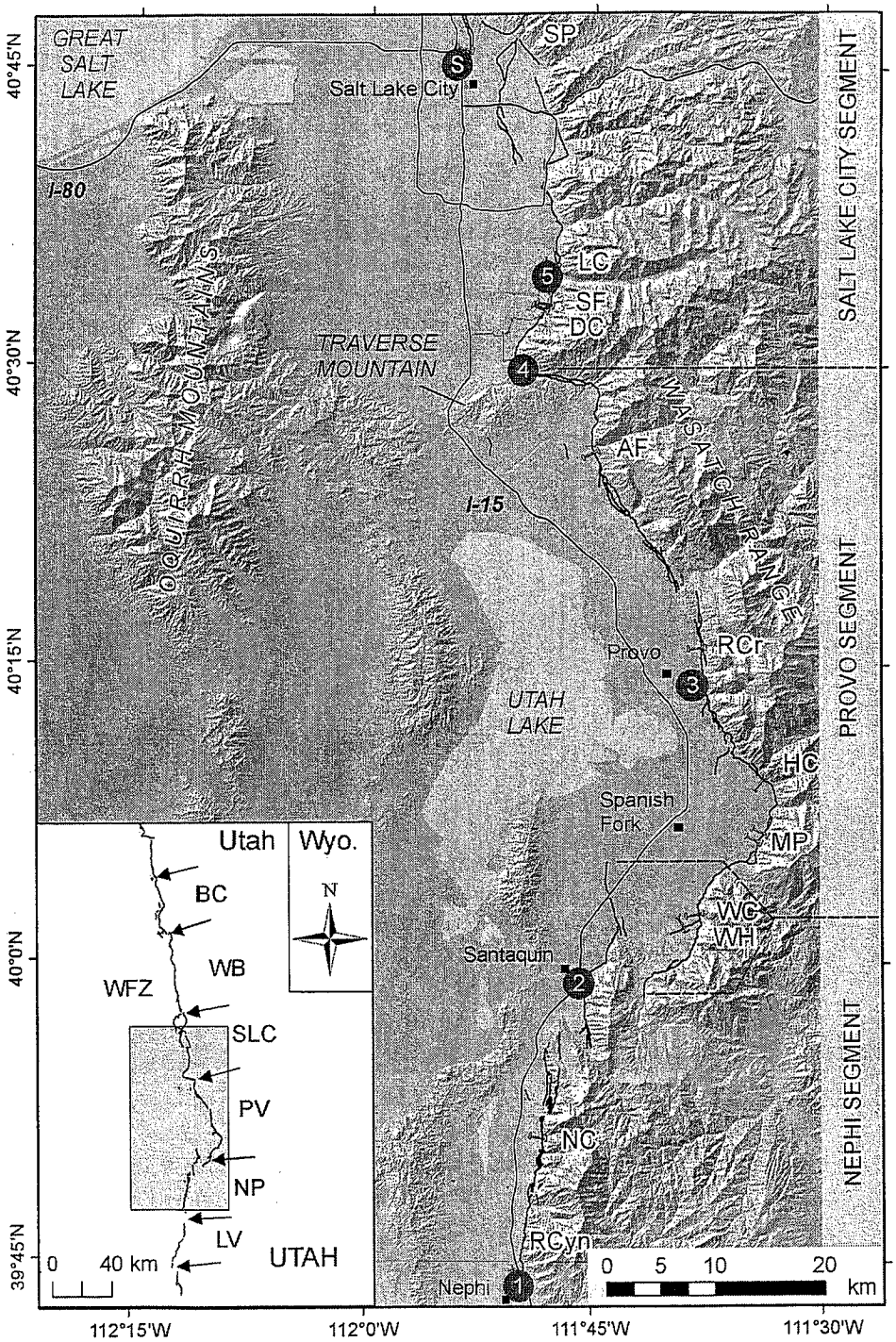

Figure 1. Shaded-relief map of the Wasatch Front with trace of the Wasatch fault (from Black et al., 2003), the Salt Lake City, Provo, and Nephi fault segments, and the locations of paleoseismology trenches. SP—Salt Palace; LC—Little Cottonwood Canyon; SF—South Fork Dry Creek; DC—Dry Gulch; AF—American Fork Canyon; RCr—Rock Creek; HC—Hobble Creek; MP—Mapleton; WC—Water Canyon; WH—Woodland Hills; NC—North Creek; and RCyn—Red Canyon). Field trip starting location (S) and stops 1 through 5 are labeled and marked by black dots. Inset map shows Wasatch fault zone (WFZ) and six central segments: BC—Brigham City; WB—Weber; SLC—Salt Lake City; PV—Provo; NP—Nephi; LV—Levan.

observations, possibly indicating the accommodation of strain by aseismic processes (Chang and Smith, 2002). Direct comparisons between horizontal rates of extension determined from geodetic data and vertical tectonic rates estimated by geologists requires knowledge of the fault's subsurface dip, which is a challenging and unresolved problem.

The subsurface geometry of the Wasatch fault has become a topic of discussion and controversy ever since G.K. Gilbert (1928) concluded that the fault dipped between 30° and 40° with an average dip of ~33°. Gilbert (1928) based his conclusion on the geometry of exposed fault surfaces and breccia zones exposed along faceted mountain fronts. He emphasized that the more

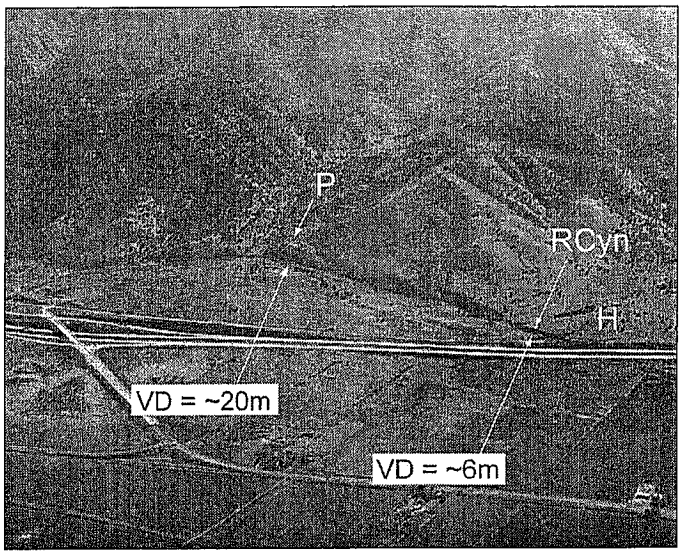

Figure 2. The Red Canyon fault scarp locality near the southern end of the Nephi segment of the Wasatch fault. The view is toward the east with I-15 in the middle ground. Note the increase in vertical displacement (VD) across the scarp from ~6 m on the Holocene alluvial surface (H) to ~20 m across the late Pleistocene fan remnant (P). RCyn—Red Canyon fault trench site (Jackson, 1991).

steeply dipping faults beneath piedmont scarps were probably high-angle splays that emanated and propagated upward from the main fault surface at shallow depths. Subsequent work has shown that Gilbert's (1928) observations remain valid. However, few subsurface data have been obtained in the intervening years despite the advent of reflection seismology, and few drill holes have penetrated the fault at depth. An exploration well penetrated the fault near Brigham City where the fault dips ~45° west (W.A. Yonkee, 2005, personal commun.). Published reflection-seismic data across the Wasatch fault are 1970s in vintage that are difficult to interpret and mostly provide evidence for the dips of Tertiary basin sediments (Smith and Bruhn, 1984). Recent geodetic measurements suggest creep on a low-angle fault or shear zone at depths of 10 km to 15 km based on numerical modeling (W.L. Chang, 2005, personal commun.). The fault-dip angle at shallower levels is better constrained, based on the attitude of exposed fault surfaces, which vary from moderate (30–40°) to more steeply dipping at some localities (Harris et al., 2000).

Historical seismicity surrounding the Wasatch fault is of particular interest both for exploring the structure and geodynamics of the fault and for detecting changes in seismicity that may precede a large earthquake. The seismicity reveals little about the subsurface structure of the fault. Earthquakes are small- to moderate-magnitude events that are scattered over a broad area. In fact, most earthquakes are located beneath the Wasatch Range to the east of the fault, rather than beneath basins in the hanging wall (Arabasz and Julander, 1986; Arabasz et al., 1979, 1992). Where concentrations of earthquakes do occur in the hanging wall, they form narrow east-west–trending belts that extend westward along segment boundaries.

FIELD TRIP

Stop 1: Red Canyon Fault Scarp—Nephi Segment

Travel Directions to Stop 1

Depart from the Salt Palace Convention Center and drive south on West Temple to 500 South. Turn right (W) on 500 South and enter the I-15 freeway driving south toward Provo and Las Vegas. Proceed south for 81 mi to Exit 228 for Nephi, Utah. After exiting, turn left (E) and proceed over the freeway and then right (S) onto the frontage road that parallels the freeway. Proceed south for 0.8 mi and park in front of the corral.

Background

The Nephi segment consists of fault scarps extending 42 km from Nephi to north of Payson along two distinct strands: the 17-km-long Santaquin strand and 25-km-long Nephi strand (Machette et al., 1992; DuRoss and Bruhn, 2005; Fig. 3). The northern Santaquin strand bounds the west side of Dry Mountain, and the southern Nephi strand bounds the Wasatch Range east of Juab Valley. A ~6-km-long, northeast-striking cross fault connects the Nephi and Santaquin strands (Machette et al., 1992; Harty et al., 1997; DuRoss, 2004). DuRoss (2004) found no evidence of Holocene or late Pleistocene displacement along the cross fault, but heavy vegetation and landslides may obscure late Quaternary displacement. The Nephi segment is separated from the Provo segment to the north by a 4.5–9-km-wide en echelon right step, and from the Levan segment to the south by a 15-km gap in Holocene and latest Pleistocene surface faulting (Hylland and Machette, 2004).

The stop at Red Canyon provides an opportunity to view a multiple-event fault scarp that increases in height where it crosses from Holocene to late Pleistocene alluvial fan surfaces (Fig. 2). Fault slip rates estimated from trenching of the Holocene fan and scarp-diffusion modeling of the fault scarps on a late Pleistocene fan remnant indicate that earthquake recurrence may have been temporally clustered, with a higher rate of activity during the Holocene (Machette et al., 1992; Mattson and Bruhn, 2001; DuRoss and Bruhn, 2005).

Fault-Scarp Geomorphology and Slip Rate

Nonlinear scarp-diffusion modeling simulates the diffusive erosion (e.g., by rain splash and soil creep) of the upper half of a measured scarp profile to determine the time at which surface displacement began, or the scarp initiation time (Andrews and Bucknam, 1987; Mattson and Bruhn, 2001; DuRoss and Bruhn, 2005). The diffusion models used for the Nephi-segment scarp profiles used a diffusivity constant calibrated with Bonneville shoreline and fault-trench data (Mattson and Bruhn, 2001), and accounted for geologic and scarp-profile instrumentation uncertainty by running numerous simulations with randomized

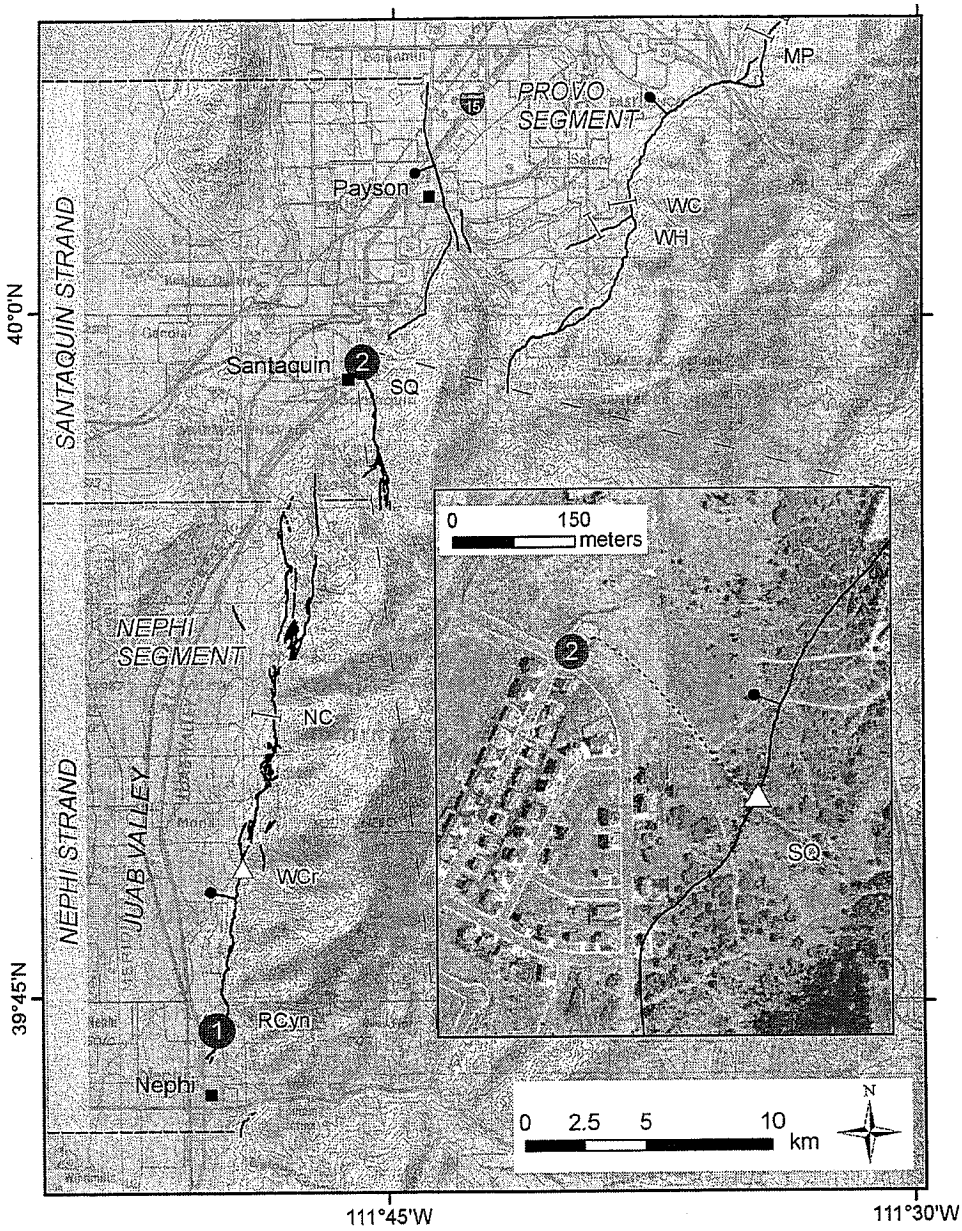

Figure 3. Nephi segment of the Wasatch fault, showing the Nephi and Santaquin fault strands and locations of previous paleoseismology trenches (annotations as per Fig. 1) and 2005 trench sites (white triangles: SQ—Santaquin site; WCr—Willow Creek site). Inset figure shows location of Stop 2. Solid black line indicates Wasatch fault trace; ball and bar on downthrown side (Machette, 1992; Harty et al., 1997; Black et al., 2003).

model parameters for each profile (DuRoss and Bruhn, 2005). Following the simulations, DuRoss and Bruhn (2005) calculated the mean vertical displacement and best-fit scarp initiation times, and formulated multiple rupture scenarios for the Nephi segment by integrating fault-trace and existing paleoseismic information. DuRoss and Bruhn (2005) calculated slip rates based on the scarp-displacement data and rupture scenarios, dividing the vertical displacement associated with a single earthquake by the elapsed time since the previous event, or in the case of multiple earthquakes, the average vertical displacement per event divided by the average recurrence interval between events. Slip rates calculated by Mattson and Bruhn (2001) include the elapsed time since the most recent earthquake and are referred to as open-ended rates.

Fault-scarp profiles and trench data (Jackson, 1991) indicate that vertical displacement across the fault scarp near Red Canyon increases from ~6 m on a Holocene alluvial fan surface to 20 m on the late Pleistocene fan remnant (Fig. 2). A fault trench excavated across the 6-m scarp revealed evidence for three earthquakes in the past 5–6 ka (Jackson, 1991) and a vertical slip rate of 0.6–1.0 mm/yr, based on scarp displacement, thickness of colluvial-wedge deposits, and earthquake timing (Harty et al., 1997; Lund, 2005). Surface displacement associated with these Holocene earthquakes is localized along the base of the 20-m scarp farther north, where there is an abrupt increase in slope angle along the lower part of the scarp's topographic profile (Mattson and Bruhn, 2001). The 20-m scarp may represent at least nine

surface-faulting earthquakes, assuming an average 1.8 ± 0.4 m of vertical displacement per event, based on the preferred fault-rupture scenario of DuRoss and Bruhn (2005).

Topographic profiling and scarp-diffusion modeling of the 20-m and 6-m scarps indicate that displacement across the late Pleistocene alluvial fan surface initiated at ca. 70 ka, yielding an open-ended slip rate of 0.4 mm/yr, less than one-half of the Holocene open-ended slip rate (1.3 mm/yr since 4.3 ka, based on diffusion modeling), possibly due to earthquake clustering during the Holocene (Mattson and Bruhn, 2001). DuRoss and Bruhn (2005) modeled the initiation time of similar scarps elsewhere along the Nephi segment, and calculated a late Pleistocene slip rate of 0.2 mm/yr (based on scarp displacement that occurred between 10–15 ka and 48–59 ka), in contrast to a Holocene slip rate of 0.5–0.7 mm/yr.

The variations in slip rate determined at Red Canyon and along the Nephi segment depend on the scarp-modeling assumption that surface displacement accumulates along a single fault beneath the middle of the fault scarp (Mattson and Bruhn, 2001). This assumption needs to be reconsidered if preliminary results of our recent seismic-imaging experiments are valid. The seismic reflection image shows three faults displacing Quaternary deposits near the top, middle, and base of the 20-m scarp (Fig. 4). Subsurface imaging does not yet allow us to discriminate between rupture scenarios with distributed faulting on two or more of the buried faults during single earthquakes versus the possibility that fault activity migrated toward the base of the scarp with time. These potential scenarios are critical to properly interpreting the evolution of the scarp profile when solving for slip rate and the time of scarp initiation on the late Pleistocene fan.

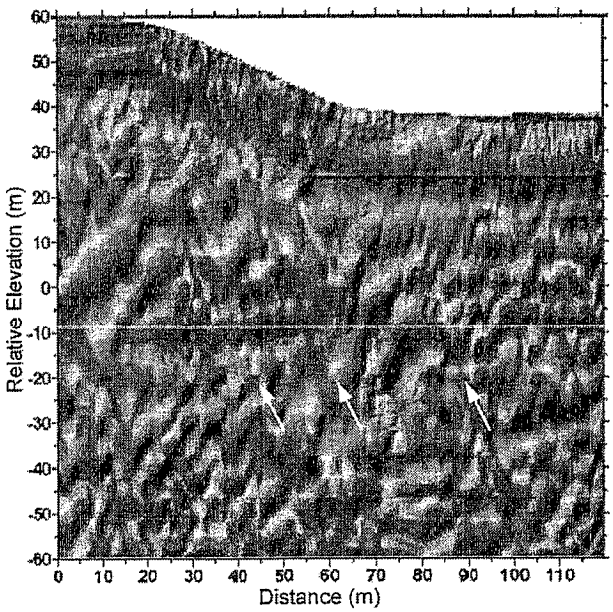

Figure 4. Seismic reflection image of the 20-m scarp at Red Canyon. Three faults are inferred beneath the top, middle, and base of the scarp (white arrows). The seismic section crosses the scarp near the ~20 m vertical displacement annotation in Figure 2. Data collection and processing provided by T. Crosby, University of Utah, using 72-fold CMP reflection processing with statics corrections for elevation and anomalous near-surface velocity.

Stop 2: Nephi Segment Fault Trench

Travel Directions to Stop 2

Return to I-15 and proceed north to the Santaquin exit (244). Turn right (E) at the end of the exit ramp and continue north on the frontage road for 0.7 mi. Turn right (NE) into a residential subdivision and continue 0.1 mi to a small city park. Park here and walk ~200 m SE along a small stream channel to the Wasatch fault (Fig. 3).

Introduction

In May of 2005, the Utah Geological Survey (UGS) and U.S. Geological Survey (USGS) excavated trenches at two sites along the Nephi segment to develop information on the timing and recurrence of earthquakes and segmentation of surface faulting. The sites include the Santaquin site (UGS), ~2 km east of Santaquin, and the Willow Creek site (USGS), ~8 km north of Nephi (Fig. 3). At Stop 2 we will visit fault trenches at the Santaquin site, located along the northern part of the Nephi segment near the mouth of Santaquin Canyon. At the site, prehistoric surface faulting has vertically displaced a late Holocene alluvial fan surface 2.5 m down-to-the-west, making it an ideal location to investigate the most recent surface faulting on the northern part of the Nephi segment. Because this field trip guide was written before excavation of the Santaquin trenches, we herein provide background information and discuss the reasons for the trench investigations.

Background

The Nephi segment has an extensive record of latest Quaternary surface faulting along its northern and southern fault strands but arguably the most poorly constrained earthquake chronology of the central, active segments of the Wasatch fault (Lund, 2005). Fault-scarp diffusion analyses along the Nephi segment indicate that at least six large-magnitude (average 6.5–7.1) earthquakes have ruptured all or part of the segment since ca. 12 ka (DuRoss and Bruhn, 2005). Most multiple-event scarps along the segment have <10 m of vertical displacement, although scarps on the oldest (~late Pleistocene) alluvial fans and landslides indicate a long history of earthquake activity with 11–25 m of displacement over the past several tens of thousands of years (DuRoss, 2004). Despite the long record of earthquakes preserved along the fault trace, trench studies (Hanson et al., 1981; Jackson, 1991) have identified only three poorly constrained mid- to late Holocene earthquakes on the southern part of the segment, supporting the need for additional fault trench investigations.

The motivation for new trenching along the northern and southern parts of the Nephi segment is that understanding the fault rupture parameters (e.g., timing, displacement, and extent)

for the individual fault strands is critical to resolve the overall earthquake behavior of the Nephi segment. In addition, paleoseismic data for the segment are presently (April 2005) limited to the Nephi strand and poorly constrain three surface-faulting earthquakes. Regional scarp analyses suggest a potential for both partial and multi-segment ruptures along the Nephi segment (DuRoss and Bruhn, 2005), but seismic-hazard analyses assume the two strands form a single segment, and as a result rely on the poorly constrained earthquake record from Nephi strand fault trenches. Thus, the UGS and USGS excavated trenches near Santaquin and Willow Creek to (1) clarify the history of paleoearthquakes on the Nephi strand (Willow Creek site), (2) determine the timing of paleoearthquakes on the Santaquin strand (Santaquin site), (3) accurately characterize the seismic-source potential of the Nephi segment, and (4) compare the Nephi segment paleoearthquake parameters (timing, displacement, recurrence) with those for the adjacent Provo and Levan segments.

Information on earthquake timing obtained at the Santaquin trench site should resolve both the nature of the Nephi-Provo segment boundary and the relation of the Santaquin strand to the Nephi strand, when compared with new paleoseismic data developed at Willow Creek. Resolving the individual rupture histories of the two strands is important, as asynchronous ruptures would result in more frequent moderate to large magnitude earthquakes, whereas synchronous ruptures of the strands would generate less frequent but larger earthquakes. Also, simultaneous ruptures of the Provo segment and Santaquin strand of the Nephi segment would create larger magnitude earthquakes than previously expected. Ultimately, the new trench information will serve to refine fault segmentation and seismic hazard models for the Wasatch fault, and improve our understanding of fault segments as individual and combined seismic sources.

Earthquake Chronology

As part of a review of paleoseismic data for Quaternary faults in Utah, Lund (2005) reported a consensus earthquake chronology for the Nephi segment (Table 1) and described the earthquake-timing information on the Nephi segment as the most poorly constrained of the five active central segments of the Wasatch fault. This Nephi segment chronology is based on fault trench studies at North Creek (Hanson et al., 1981) and Red Canyon (Jackson, 1991) on the Nephi strand, which identified evidence for three surface-faulting earthquakes since the middle Holocene (based on fan alluvium ^{14}C dated at ca. 5300 cal yr B.P. by Bucknam, 1978). However, the investigations produced conflicting sets of numerical ages, and as a result, significantly different earthquake chronologies exist depending on how the age data are treated. For example, at North Creek, five ^{14}C ages for a soil formed on top of the event Y colluvial wedge cluster into two groups between 1400 and 1650 ^{14}C yr B.P. and between 3600 and 3900 ^{14}C yr B.P. Hanson et al. (1981) preferred the older sets of ages as representative of the soil and the minimum limit on the timing of event Y. At the Red Canyon site over 12 km south of the North Creek site, Jackson (1991) selected ^{14}C and thermoluminescence ages for the two most recent events that were consistent with the North Creek data. He extrapolated the age of the North Creek fan alluvium (Bucknam, 1978) in order to constrain the timing of event X at Red Canyon.

DuRoss and Bruhn (2005) formulated multiple earthquake scenarios for the Nephi segment based on scarp diffusion modeling, scarp trace, and vertical displacement data (Table 2; Fig. 5). The preferred earthquake history includes six ruptures on the Nephi segment since the latest Pleistocene, having an average vertical displacement per event of 1.8 m. Two events ruptured the entire Nephi segment (both Nephi and Santaquin strands simultaneously), and four younger events ruptured only one of the fault strands. The earthquake time ranges are qualitative estimates, based on diffusion model and fault-trench data uncertainties. The broad ranges and possible partial-segment ruptures illustrate the need for additional paleoseismic data to test and constrain the timing of events along both fault strands.

Earthquake Rupture Patterns

Partial segments. Based on the earthquake timing (from both fault-trench and diffusion modeling data), along-strike changes in scarp morphology and displacement, and surface

TABLE 1. CONSENSUS EARTHQUAKE TIMING FOR THE NEPHI SEGMENT

Event	Consensus time range
Z	<1 ± 0.4 ka, but possibly as young as 0.4 ± 0.1 ka
Y	ca. 3.9 ± 0.5 ka
X	>3.9 ± 0.5 ka, <5.3 ± 0.7 ka

Note: From Lund (2005).

TABLE 2. PREFERRED EARTHQUAKE CHRONOLOGY FOR THE NEPHI SEGMENT BASED ON SCARP-DIFFUSION MODELING AND FAULT-TRENCH DATA.

Event*	Preferred time range
Z^S	0.4–0.6 ka (partial rupture—Santaquin strand?)
Z^N	1.0–1.4 ka (partial rupture—Nephi strand?)
Y^S	2.0–3.0 ka (partial rupture—Santaquin strand?)
Y^N	ca. 3.9–4.0 ka (partial rupture—Nephi strand?)
X	ca. 5.2–7.0 ka
W	ca. 10-15 ka

Note: Modified from DuRoss and Bruhn (2005).
*Events Z^S and Y^S are based on diffusion-modeling data. Events Z^N, Y^N, and X are based on both diffusion-modeling and fault-trench data. Event Y^N is based primarily on paleoseismic-trench data due to a paucity of scarps recording only the youngest two events on the Nephi strand. Event W is inferred from displacement across Bonneville shoreline.

fault–trace geometry, DuRoss and Bruhn (2005) suggested that the 4.2- to 7-km-wide Nephi-Santaquin fault-strand step-over may impede small ruptures on the individual strands, evidenced by the proposed timing and geometry of rupturing along the two strands (DuRoss and Bruhn, 2005). Along both strands, the youngest fault rupture traces bifurcate and the vertical displacements decrease abruptly toward the strand step-over, indicating rupture impediment. The youngest two ruptures on each fault strand are morphologically and structurally distinct across the strand step-over. The youngest displacement on the Santaquin strand is limited to the southern half of the strand where 1.0 m of displacement occurred at ca. 0.4–0.6 ka, based on scarp diffusion modeling (DuRoss and Bruhn, 2005). In contrast, the youngest rupture on the Nephi strand occurred at ca. 1.0–1.4 ka with 1.7 m of displacement, based on diffusion modeling and fault trench data. Scarp initiation times suggest that the next oldest event on the Santaquin strand occurred at ca. 2.0–3.0 ka, in contrast to the event on the Nephi strand estimated at ca. 3.9–4.0 ka, based dominantly on fault trench data.

Multiple segments. The Santaquin strand may also rupture due to coseismic stress interaction with paleoearthquakes along the Provo segment to the north (DuRoss and Bruhn, 2005). Provo segment ruptures propagating toward the fault's southern tip would need to transfer slip across a 4.5–6.5-km distance to rupture the Santaquin strand in Santaquin Canyon or a ~9-km distance to rupture the northern part of the Santaquin strand (Fig. 3). DuRoss and Bruhn (2005) reported that the youngest ruptures on the Santaquin strand are mostly limited to Santaquin Canyon (~7 km long; Figs. 3 and 5) and scarps associated with the events initiated at ca. 0.5 ka and ca. 2.6 ka based on diffusion modeling. In comparison, fault trench studies on the Provo-segment identified large displacement ruptures along the entire fault, the youngest of which occurred ca. 0.6 and ca. 2.85 ka (Lund et al., 1991; Lund and Black, 1998; Lund, 2005). Based on mechanical modeling, a 60-km-long rupture of the Provo segment would induce the greatest Coulomb failure stress change on the southern half of the Santaquin strand (four bars at 10 km depth; Chang, 1998), decreasing significantly to the south along the Nephi strand. Conversely, DuRoss and Bruhn (2005) considered the Payson salient to be an effective barrier to ruptures propagated on the Nephi segment, based on the fault geometry, distribution of slip, and minor stress change

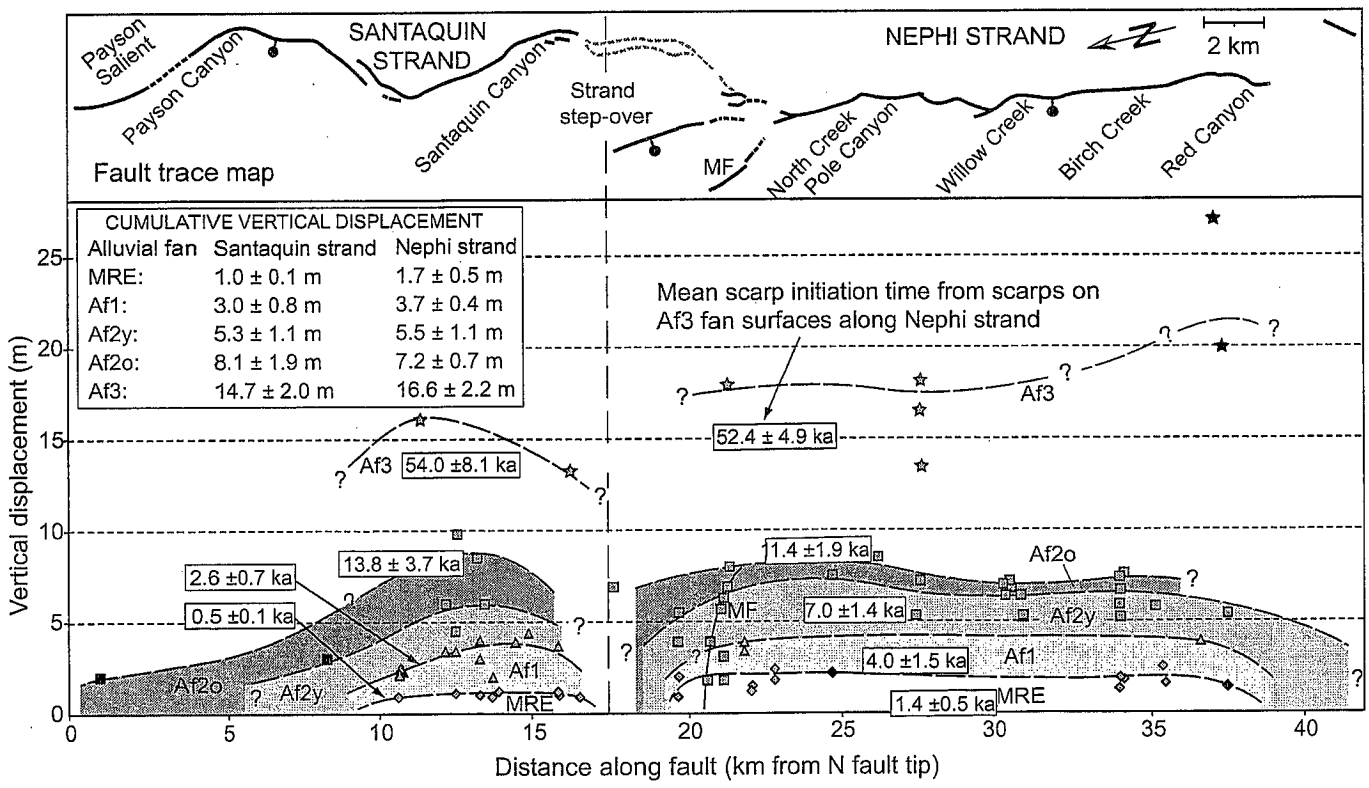

Figure 5. Distribution of vertical displacement along the Nephi segment from displaced alluvial fan surfaces. Diamonds—MRE (most recent event); Af—alluvial fan: triangles—Af1; squares—Af2 (y—younger, o—older); stars—Af3 (modified from DuRoss and Bruhn, 2005). Gray shapes and inset chart of vertical displacement data from scarp-profile surveying (DuRoss and Bruhn, 2005); black shapes from Hanson et al. (1981), Jackson (1991), Machette (1992), and Mattson and Bruhn (2001). Mean scarp initiation times (±1σ) from scarp-diffusion modeling (DuRoss and Bruhn, 2005). MF—Mendenhall fault.

(~1.8 bars; Chang, 1998) imposed on the southern Provo segment due to a Nephi segment earthquake.

Stop 3: Provo Segment of the Wasatch Fault and the Seven Peaks Fault Scarp

Travel Directions to Stop 3

Return to I-15 and drive north 18 mi to Exit 263 (Utah Hwy 189). Proceed north on University Avenue for 1.5 mi and then turn right onto 300 South. Continue east on 300 South for 0.8 mi to the intersection with 900 E. Turn left at 900 E and drive 0.3 mi north to East Center Street. Turn right onto East Center St. and drive 0.1 mi to Seven Peaks Blvd. Proceed northward for 0.3 mi to the Seven Peaks Resort. An exposure of the Wasatch fault is located at the base of the mountain just east of the resort headquarters.

Provo Segment of the Wasatch Fault

The Provo segment of the Wasatch fault bounds the eastern side of Utah Valley (Figs. 1 and 6). It has a 60-km-long surface rupture trace that extends from the Traverse Mountains south of Salt Lake City to Payson. The most recent major earthquake (moment magnitude [M_w] ~7.1) along the Wasatch fault occurred along the Provo segment between 500 and 700 yr B.P., based on fault trenching (Lund et al., 1991; Machette, 1992; Lund and Black, 1998). Scarps from this earthquake are still well preserved in places. Displacement across the Bonneville shoreline (16.8–18 ka, based on radiocarbon dating; D. Currey, written commun. *in* Lund, 2005) varies along the segment from 15 to 26 m near American Fork (Machette, 1992) to 40–45 m near Hobble Creek (Swan et al., 1980; Machette et al., 1992; Lund, 2005), which yields long-term (open-ended) slip-rate estimates of 0.8–1.5 mm/yr and 2.2–2.7 mm/yr, respectively (Machette, 1992; Lund, 2005). Contemporary horizontal loading rates for the fault vary from 2 to 4 mm/yr, based on geodetic measurements (EDM and GPS) over the past few decades (Martinez et al., 1998; Friedrich et al., 2003). Differences between these rates can be accounted for either by movement along a low-angle slip surface or by viscoelastic behavior, in which a significant amount of the viscous component is not recovered during coseismic deformation (Harris et al., 2000).

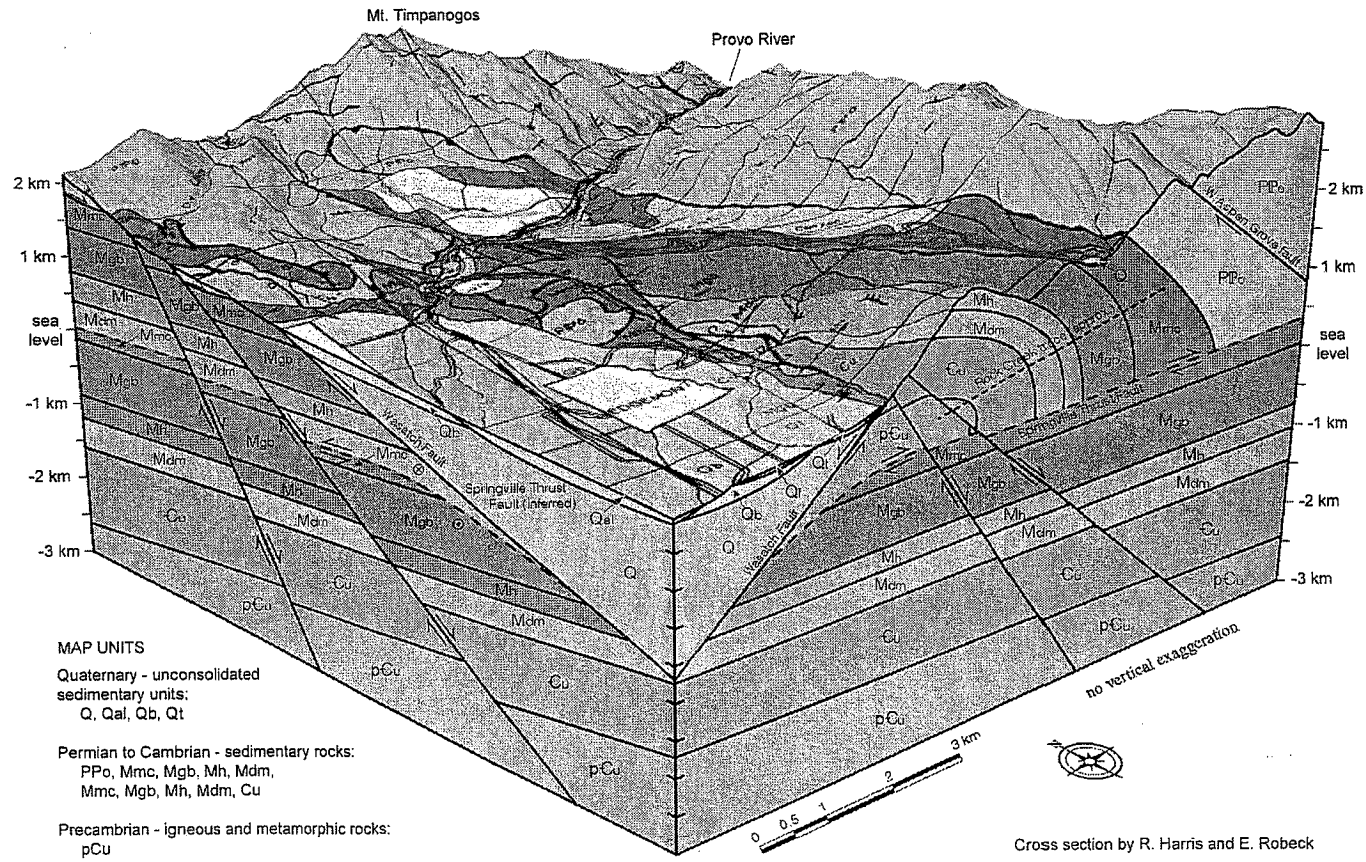

Figure 6. Block diagram of the Wasatch Front and Utah Valley near Rock Canyon (E-W line) and Lindon (N-S) line. The Wasatch fault cuts through the back limb of the Rock Canyon anticline, which plunges north. The ramp associated with this fault propagation–type fold may have been reactivated as part of the Wasatch fault. A series of antithetic faults with top-down-to-the-east slip offset the folded rocks in the footwall. Cross section constructed by R. Harris and E. Robeck.

The footwall of the Provo segment consists of mostly Paleozoic and locally Precambrian sedimentary rocks (Fig. 6). In most cases these rocks form part of the gently dipping back limb of the east-verging Nebo-Charleston thrust sheet. Structural reconstructions indicate that the Wasatch fault is parallel to, and may have reactivated thrust ramps associated with, the Nebo-Charleston thrust (Smith and Bruhn, 1984). Many of the gently dipping sedimentary rocks in the footwall are tilted up to 40° west by drag along the Wasatch fault (Fig. 7). The break in slope on the footwall evident throughout the Provo segment marks the position of the erodable Upper Mississippian to Lower Pennsylvanian Manning Canyon Shale, in contrast to the cliffs of overlying Pennsylvanian to Permian Oquirrh Group limestone and sandstone (Fig. 6).

The hanging wall of the Provo segment consists mostly of blocks of Paleozoic rocks and of upper Cenozoic basin fill. Most of the blocks consist of Mississippian limestone, in some cases displaced thousands of meters downward from their footwall source (Fig. 6). Middle Miocene to modern basin-fill deposits are estimated to be a maximum of 4 km thick from drilling and gravity surveys (Mabey, 1992). The stratigraphic thickness of hanging-wall rocks below the basin fill and above the Wasatch fault is estimated at ~10 km (Hintze, 1988). This implies that there has been at least 10 km of vertical displacement along the fault since the middle Miocene. The bedrock part of the hanging wall emerges from the basin fill to the west of Utah Valley to form Lake Mountain. This configuration is consistent with hanging wall rotation associated with listric fault geometry and half-graben development.

Reconstructions of the prefaulting stratigraphy suggest that the footwall is exhumed by ~6 km, but this amount of exhumation is much greater than the estimated thickness of basin fill. Either there was a fluvial outlet for sediment to leave the hanging-wall basin, or much of the exhumation was accomplished by low-angle extensional faulting rather than erosion.

Seven Peaks Fault Scarp

Excavation for a ski lift, as part of the abandoned Seven Peaks Ski Area at the base of "Y" Mountain, exhumed part of a slip surface in the core zone of the Wasatch fault at Stop 3 (Fig. 8). The slip surface is less than 1 m thick and is composed mostly of polished limestone breccia. Several meters of pulverized carbonate gouge surround the slip surface. Lenses of limestone wall rock are scattered throughout the gouge.

The slip surface strikes N-S and dips 42–46°W. It is characterized by a series of steeply dipping corrugations with wavelengths of around a meter, which have slickenside lineations on them. The lineations have a rake of 85–88°S and are up to 160 cm in length, with the majority measuring 30–60 cm in length. Most lineations widen and shallow down dip in a wedge-shaped fashion. Secondary tensile fractures (stretch marks) taper downward into the surface and are mostly horizontal. The longest striae are similar in length to the minimum amount of vertical displacement per event observed in fault trenches across the Provo segment (~1.6–3.3 m; Swan et al., 1980; Machette et al., 1992; Lund and Black, 1998). If the grooves and displacements are from one coseismic event that ruptured the entire Provo segment, it would

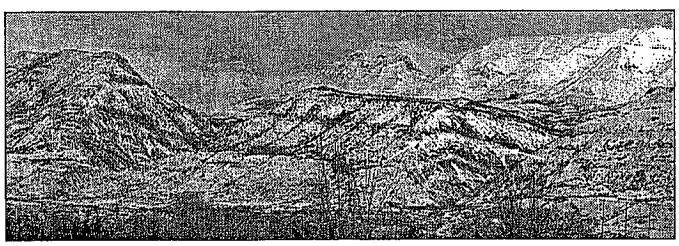

Figure 7. Fault drag along the Provo segment (between white arrows). Resistant layers of Mississippian limestone are folded down into the fault. Immediately adjacent to the fault, intervening shale between the limestone layers has been removed from between the resistant units and incorporated into the gouge zone. Mount Timpanogos rises in the distance above a strike valley formed by erosion of the Manning Canyon Shale.

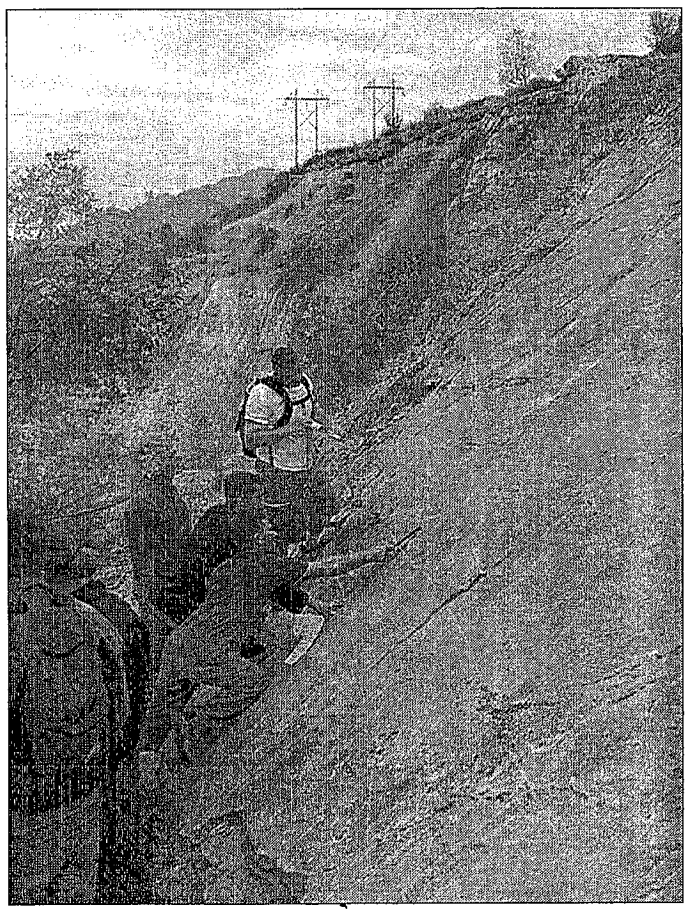

Figure 8. Slip surface and architecture of the Seven Peaks fault scarp at Stop 3. Slip surface is polished carbonate-clast breccia with dip-parallel slickenlines. Material in the distance consists of fault gouge (dark gray), blocks of limestone (light gray), and displaced Lake Bonneville deposits (bedded gray units at base).

have produced an earthquake with a M_w ~7.1 (Chang and Smith, 2002). Lee and Bruhn (1996) measured the roughness of the fault surface at this site and concluded that the topography of the fault surface was partly controlled by processes associated with coseismic slip of 1–2 m per earthquake.

Stop 4: Salt Lake–Provo Segment Boundary at Corner Creek

Travel Directions to Stop 4

Return to I-15 from Stop 3 and proceed northward 22 mi to Exit 288 for Utah Hwy 140. Continue for 0.5 mi to the intersection with Highland Drive. Turn right heading north and east on Highland for 2.7 mi to the intersection of Rambling Road. Turn right onto Rambling Road and proceed up the hill for 0.9 mi, passing through the roundabout onto Sage Hollow Drive. Continue east and uphill on Sage Hollow and onto Gray Fox Drive for 0.5 mi past the roundabout. Turn left and downhill onto Coyote Hollow Drive and park in the designated area. Walk east along the creek to exposures of the Wasatch fault.

Geologic Description

The boundary between the Salt Lake and Provo segments is a 7-km-wide jog formed by an east-trending cross fault (Fig. 9; Gilbert, 1928; Schwartz and Coppersmith, 1984; Bruhn et al., 1992). At this locality we will observe remnants of the Wasatch fault that formed at a depth of at least 11 km and at temperatures of 350–400 °C (Parry and Bruhn, 1987). The rocks are a mixture of phyllonite (mica-rich mylonite), cataclasite, and thin bands of relict pseudotachylite (frictional melt rock) that provide evidence for processes of fault creep and earthquake rupturing in the hypocentral regions of magnitude ~7 earthquakes (Parry and Bruhn, 1986; Bruhn et al., 1990; Yonkee and Bruhn, 1990).

The exhumed fault rock forms a thin carapace on the margins of the Little Cottonwood stock, an Oligocene granitic intrusion that is mostly quartz monzonite (Fig. 9). The fault segment boundary defines a roughly cylindrical structure plunging 20°–25° W-SW beneath the eastern Traverse Mountains, a bedrock ridge of Paleozoic sedimentary rocks and Tertiary volcanic rocks that extends outward from the mountain front in the hanging wall of the Wasatch fault (Fig. 9). Fault slip directions are mostly west to west-southwest based on the orientation of slickenlines and angular relations between foliation and shear surfaces preserved in the phyllonite. Although minor faults are highly variable in orientation and exhibit a broad range of slip directions, the average slip directions for the larger fault sections are consistent with a best-fit regional stress tensor having a maximum principal stress ($\sigma 1$) plunging steeply SW, a gently NNW-SSE–plunging $\sigma 2$ axis, and gently ENE-WSW–plunging $\sigma 3$ axis (Yonkee and Bruhn, 1990).

Cross sections constructed through the fault carapace reveal several distinctive zones of deformation and alteration (Fig. 10). Granite in the footwall (zone 0) is cut by widely spaced fractures that form sets of steeply dipping and subhorizontal joints, and has undergone little hydrothermal alteration. This rock grades upward into a transition zone of heterogeneously deformed and altered rock with thickness that varies from ~20 m to >200 m. The lower, or zone 1, part of this transition zone is dissected by decimeter-spaced fractures and an increase in the number

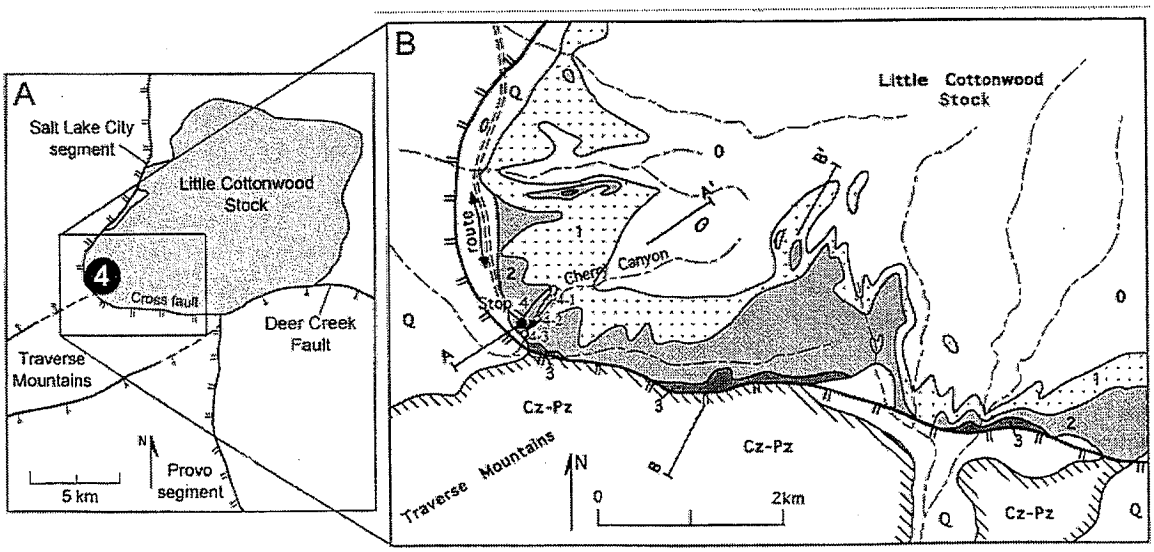

Figure 9. Map of the Salt Lake–Provo segment boundary in the Wasatch fault zone, showing (A) fault traces and location of Little Cottonwood Stock, and (B) segment boundary geology and spatial distribution of fault-zone and country rock. Map symbols 0, 1, 2 and 3 refer to rock zones described in the text. Cz–Pz—Cenozoic and Paleozoic rocks; Q—undifferentiated Quaternary deposits. The Wasatch fault trace is mapped as a thick and double hatched line. Reproduced from Evans et al. (1997) and based on work by Yonkee and Bruhn (1990).

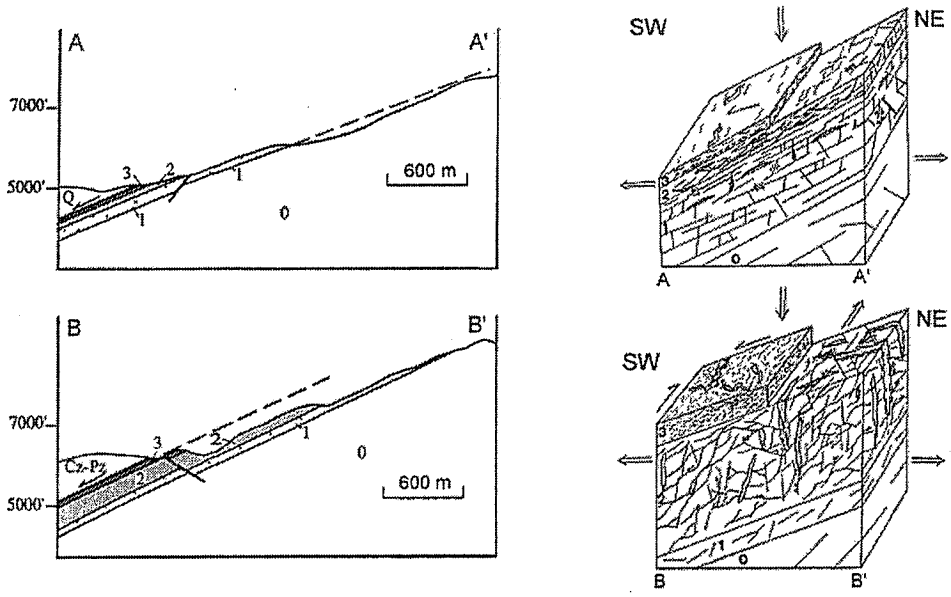

Figure 10. Structural cross sections of the Wasatch fault along lines A–A′ and B–B′ shown in Figure 9. The numbers on the variably shaded units refer to the fault rock zones discussed in the text. Block diagrams to the right side of the figure are sketches illustrating the fracture and vein patters observed in the various fault rock zones. Modified from Evans et al. (1997) and based on work by Yonkee and Bruhn (1990).

of minor faults compared to zone 0. The upper, more deformed part of the transition zone (zone 2) is characterized by variably oriented fractures with centimeter-scale spacing and many small faults. Quartz veins are common throughout this zone, most of the veins dip steeply, and many veins display evidence for repeated cracking and resealing. The quartz veins reflect episodic dilation and horizontal extension within the fault zone. The transition zone changes upward into the fault slip zone (zone 3) that is generally <10 m thick and is where most displacement occurred based on the presence of large slip surfaces and the intensity of deformation. Rocks in this zone include fault breccia, cataclasite, phyllonite, and large striated fault surfaces. Veins of partly altered pseudotachylite both cross cut and are deformed by the phyllonitic (ductile) and cataclastic (brittle) fabrics, recording alternating periods of quasiplastic creep and rapid brittle faulting, presumably caused by rupture propagation and frictional sliding and heating during earthquakes (Yonkee and Bruhn, 1990). Cataclasite dikes that were injected outward from fault surfaces also provide evidence of very rapid fracturing and material transport.

The intimate relation between hydrothermal and deformation processes within the fault zone is perhaps the most important observation to make at this locality. Hydrothermal alteration is concentrated along fracture and vein networks in the transition zone and pervades the fault-slip zone. There are two alteration mineral assemblages: (1) the oldest and most widespread is a quartz-muscovite-chlorite-epidote assemblage that formed at T >300–350 °C, and (2) a younger and spatially restricted assemblage of prehnite and clay minerals that formed at T <200 °C within the upper few km of the fault zone. Fluid inclusion data indicate transient changes in paleofluid pressure between lithostatic and hydrostatic that was presumably associated with earthquake cycles while the rocks were at depths of ~10 km (Parry and Bruhn, 1986). The evidence suggests that fracturing and hydrothermal alteration of feldspar to micaceous assemblages at temperatures of 350–400 °C dramatically weakened the granitic protolith, enhanced ductile deformation, and consequently localized shearing within the fault zone while the unaltered granite in the footwall remained undeformed. Granitic rocks located only tens of meters from the hydrothermal system were largely unaffected by chemically reactive fluids in the fault zone and by earthquake ruptures that propagated only tens of meters away.

Stop 5: The Wasatch Fault at Little Cottonwood Canyon

Travel Directions to Stop 5

Retrace route from Stop 4 to Highland Drive. Turn NE on Highland and proceed to the intersection of 1300 East. Turn north on 1300 East and continue to the Draper Parkway. Turn right (E) on Draper Pkwy, which will become 1700 East. Continue north on 1700 East to the intersection with Wasatch Boulevard. Turn east onto Wasatch Boulevard and continue east and then north to the park at the intersection of Wasatch Blvd and Little Cottonwood Canyon Road. Turn into the park for Stop 5. To return to the field trip start (Salt Palace Convention Center), proceed west on Little Cottonwood Canyon Road, which will become 9000 South, and enter I-15 driving north toward Salt Lake City. Proceed north for 11 mi to Exit 306 (600 South). After exiting, proceed east on 600 South and then turn left (N) on West Temple. Continue north for ~0.75 mi to the convention center.

Introduction

At the mouth of Little Cottonwood Canyon, a prominent glacier-carved valley in the Wasatch Range, the Wasatch fault is expressed by some of the most spectacular and complex scarps

found anywhere along its length (Fig. 11). The fault zone is up to 400 m wide and consists of prominent curvilinear and en echelon west-facing and antithetic scarps that form a major graben in glacial moraines, Lake Bonneville deposits, and alluvium (Fig. 12). Individual west-facing scarps within the zone reach heights of 35–40 m and antithetic scarps range in height from 7 to 20 m (Schwartz and Lund, 1988).

Little Cottonwood Canyon is on the Salt Lake City segment of the Wasatch fault (Fig. 1), one of ten seismogenically independent fault segments identified by Machette et al. (1992) that are distinguished by their unique paleoearthquake chronologies. The Salt Lake City segment is the most heavily urbanized Wasatch fault segment. Urbanization began at the north end of the segment in 1847 with the founding of Salt Lake City and has moved progressively southward over the ensuing 158 years. As a result, most fault exposures on the northern part of the segment were either destroyed or made inaccessible long before paleoseismology developed as a science. In the late 1970s when geologists first began conducting modern paleoseismic investigations on the Salt Lake City segment, they were forced by circumstances to look for sites on the southern part of the segment. However, the fault scarps at Little Cottonwood Canyon are so spectacular and instructive that they drew the attention of G.K. Gilbert, one of America's preeminent early geologists, nearly 130 years ago, thus securing for the Wasatch fault at Little Cottonwood Canyon a prominent place in the geologic history of the Basin and Range.

G.K. Gilbert

G.K. Gilbert (1843–1918) was one of the most perceptive geologists ever to work in the American West. His regional investigations of Basin and Range geology with the Wheeler Survey (1871–1874), Powell Survey (1875–1879), and U.S. Geological Survey (1879–1883) resulted in a number of scientific firsts and benchmark studies that are classics of American geologic thought. Many of his theories have withstood the test of time, notably his contributions to the understanding of mountain building processes and earthquakes in the Basin and Range Province. He was the first to recognize that faulting and not folding is the primary mechanism responsible for mountain building in the interior basins of Utah and Nevada (Gilbert, 1872, 1875). He was also the first to recognize "piedmont" scarps as evidence that the mountains are the result of incremental movement along range-bounding faults during earthquakes (Gilbert, 1875, 1890, 1928).

The fault scarps at Little Cottonwood Canyon occupy a prominent place in the development of G.K. Gilbert's theories concerning mountain building and earthquakes, and his field notes contain numerous sketches of the scarps and moraines at this location (Wallace, 1980; Hunt, 1982). Gilbert visited this locality twice in 1877 to make notes on the geology and surface-water resources and again in 1880 to spend several days mapping the geology. Gilbert (1890) mapped and profiled the glacial moraines, and mapped the fault scarps where they cross the moraines and fan deposits defining a major graben. He noted the complexity of the fault zone and that it contains opposing scarps. Based on his observations that the scarps in the moraines are higher than scarps in younger alluvial deposits, he concluded that "it is evident that the total displacement was accomplished by a series of efforts" (Gilbert, 1890, p. 347).

In 1883, confident that his theories about mountain building and earthquakes were correct, Gilbert issued an earthquake hazard warning to the residents of Salt Lake City. In an article in the Salt Lake City *Tribune* (20 September 1883) and later reprinted in the *American Journal of Science* (Gilbert, 1884), he summarized his ideas and emphasized their practical application to Utah. Gilbert's earthquake warning was remarkable for its recognition that earthquakes in the Basin and Range are unevenly distributed in space and time. He concluded that once an earthquake occurs at a particular location on a fault, it is unlikely that another will take place there until enough time has elapsed for sufficient strain to reaccumulate. He interpreted the presence of young scarps at this location, but their absence farther north, as evidence of long quiescence and strain accumulation in the Salt Lake City area, thus making that subdued section of the fault a prime candidate for a future earthquake. It was not until almost 100 years later, in 1979, that geologists pursuing the budding science of paleoseismology finally returned to Little Cottonwood Canyon to begin the arduous process of quantifying the past behavior and earthquake potential of the Wasatch fault.

Modern Paleoseismology Studies

In addition to figuring prominently in development of our early understanding of Basin and Range faulting, the Wasatch fault was also the first normal-slip fault in the world to be investigated using modern paleoseismic techniques. Much of what is now considered state-of-the-art paleoseismic practice for investigating faults was originally developed and refined at Little Cottonwood Canyon and at other sites along the Wasatch fault.

Woodward-Clyde consultants—the first paleoseismic study. Woodward-Clyde Consultants conducted the first paleoseismic study on the Salt Lake City segment in 1979. Their study was one of the first ever conducted on a normal-slip fault anywhere, and was in the Little Cottonwood graben ~200 m northeast of where we are now standing (Fig. 12). The study included excavation of four trenches and topographic profiling of the faulted Bells Canyon lateral moraine (immediately south and east of our present location). Based on stratigraphic relations in the trenches and the results of early accelerator–mass spectrometry ^{14}C dates, Woodward-Clyde concluded that there was evidence for at least two surface faulting earthquakes during the Holocene at Little Cottonwood Canyon: a penultimate earthquake that occurred shortly before 8–9 ka, and the most recent earthquake that is younger than 8–9 ka, but the timing of which could not be further constrained (Swan et al., 1981; Schwartz and Coppersmith, 1984). A critical result of the Woodward-Clyde study was the recognition of a distinct Salt Lake City segment of the Wasatch fault (Schwartz and Coppersmith, 1984).

Utah Geological Survey—South Fork Dry Creek and Dry Gulch Trench sites. Recognizing that it was unlikely that the

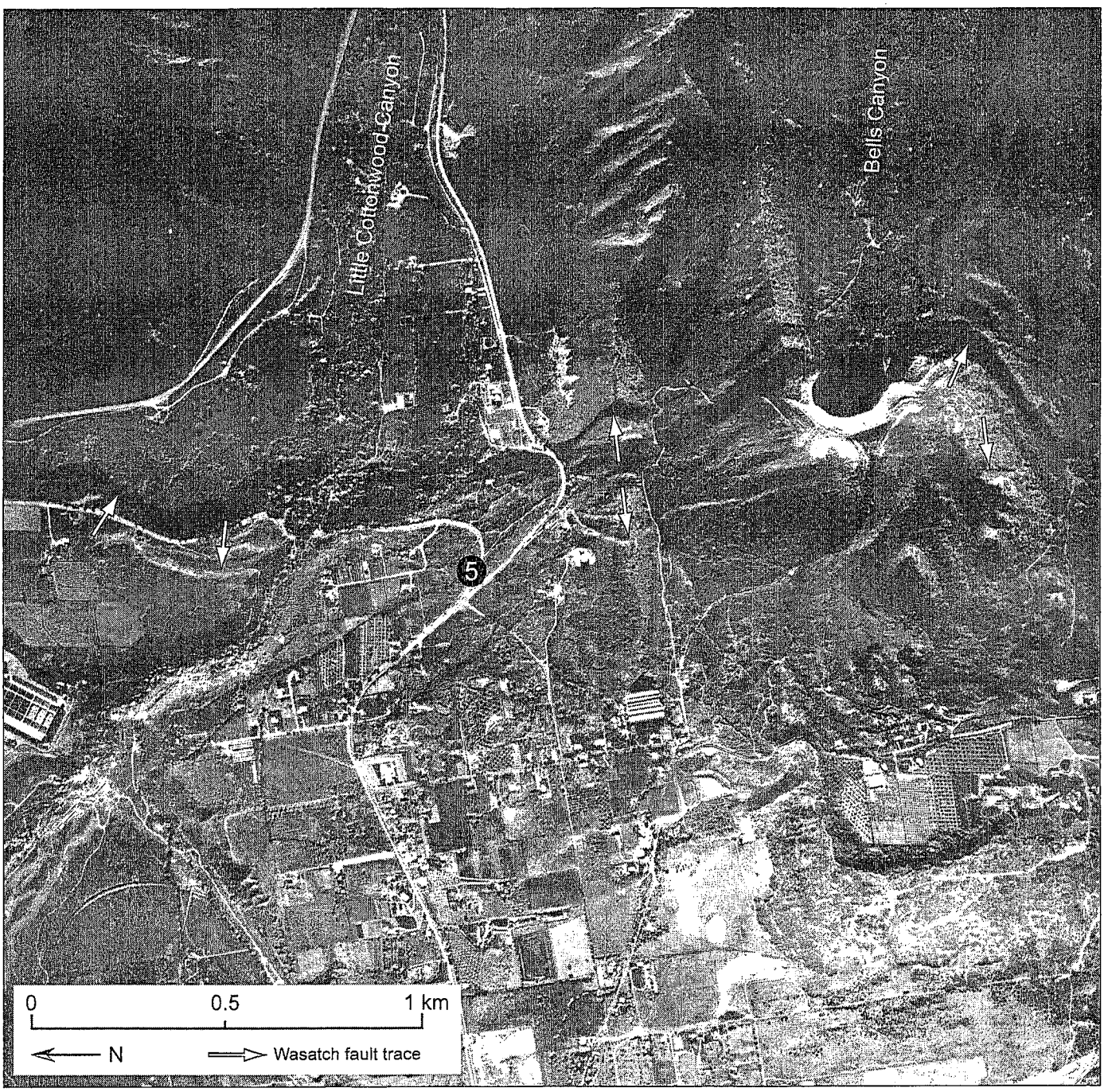

Figure 11. Low sun–angle aerial photograph showing the complexity and width of the Wasatch fault (white arrows) at the mouths of Little Cottonwood and Bells canyons and the location of Stop 5.

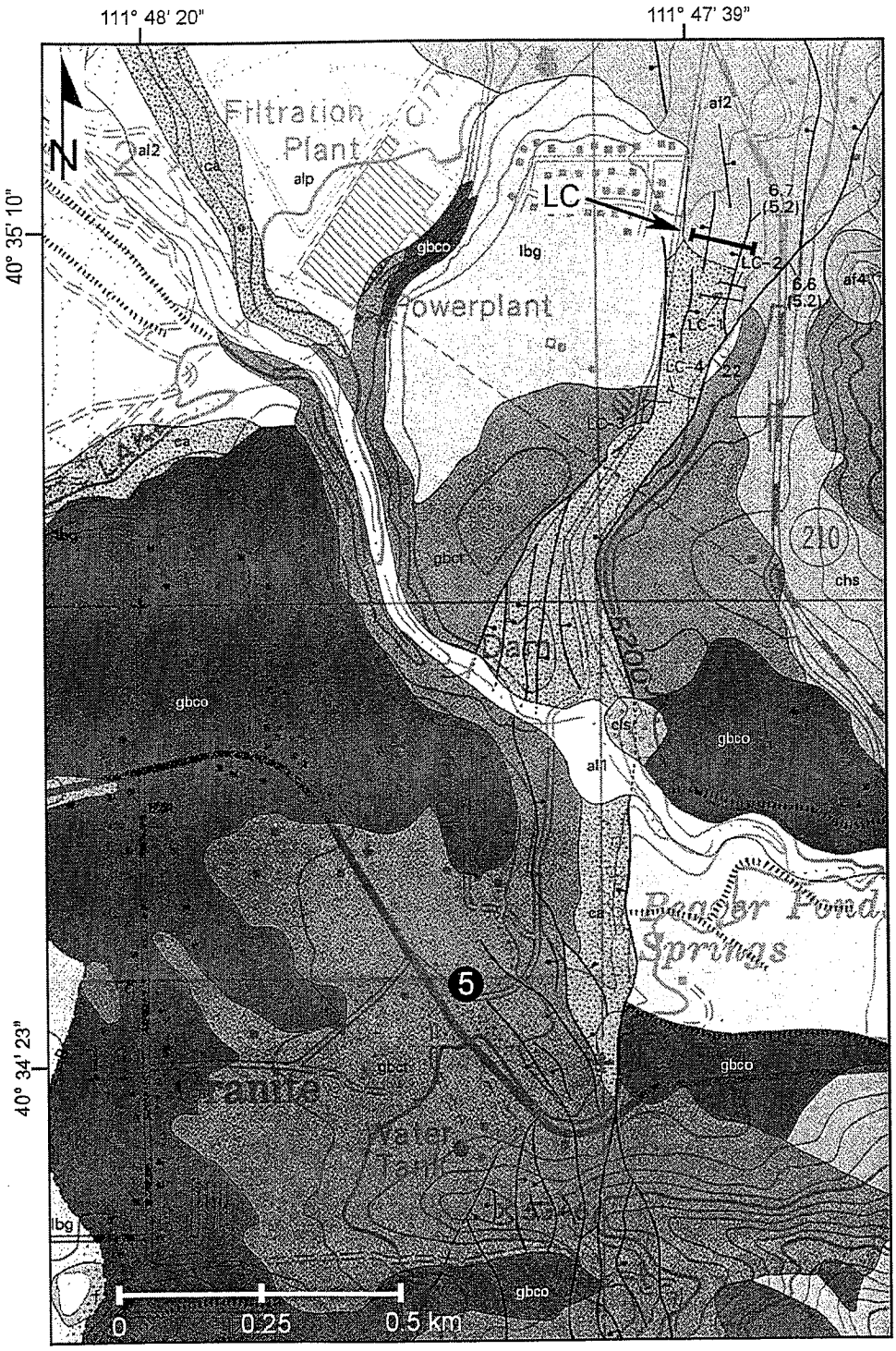

Figure 12. Surficial geologic map of the mouth of Little Cottonwood Canyon showing the Little Cottonwood megatrench site (LC) and Woodward-Clyde trenches (LC-1–4). Map units: al1, al2, and alp—stream alluvium; af2 and af4—alluvial fan deposits; chs and ca—colluvial and alluvial deposits; gbct and gbco—glacial deposits; lbg—Lake Bonneville lacustrine deposits. Modified from Personius and Scott (1992).

Woodward-Clyde paleoseismic investigation had determined a complete Holocene earthquake chronology for the Salt Lake City segment, the Utah Geological Survey, with assistance from the U.S. Geological Survey and funding from the National Earthquake Hazards Reduction Program (NEHRP), undertook a series of paleoseismic studies in the 1980s and 1990s at South Fork Dry Creek and Dry Gulch (Black et al., 1996) ~3 km south of Stop 5. The advantages of the South Fork Dry Creek and Dry Gulch sites were twofold: first, the sites were in nearly pristine condition; second, slip across the Wasatch fault was distributed across a zone roughly 400 m wide on several subparallel scarps whose heights were measured in meters rather than tens of meters, making the scarps easier to trench. The Utah Geological Survey excavated nine trenches across the fault scarps at South Fork Dry Creek and logged a consultant's trench excavated across one fault scarp at Dry Gulch.

TABLE 3. TIMING OF SURFACE-FAULTING EARTHQUAKES ON THE SALT LAKE CITY SEGMENT DETERMINED AT THE SOUTH FORK DRY CREEK AND DRY GULCH TRENCH SITES

Event	Minimum timing (cal yr B.P.)	Preferred timing (cal yr B.P.)	Maximum timing (cal yr B.P.)
Z	1100	1300	1550
Y	2100	2450	2800
X	3500	3950	4500
W	4950	5300	5750

Note: From Black et al. (1996). Earthquake timing is based on a combination of apparent mean resident time and accelerator mass spectrometer radiocarbon ages obtained from the South Fork Dry Creek and Dry Gulch trenches.

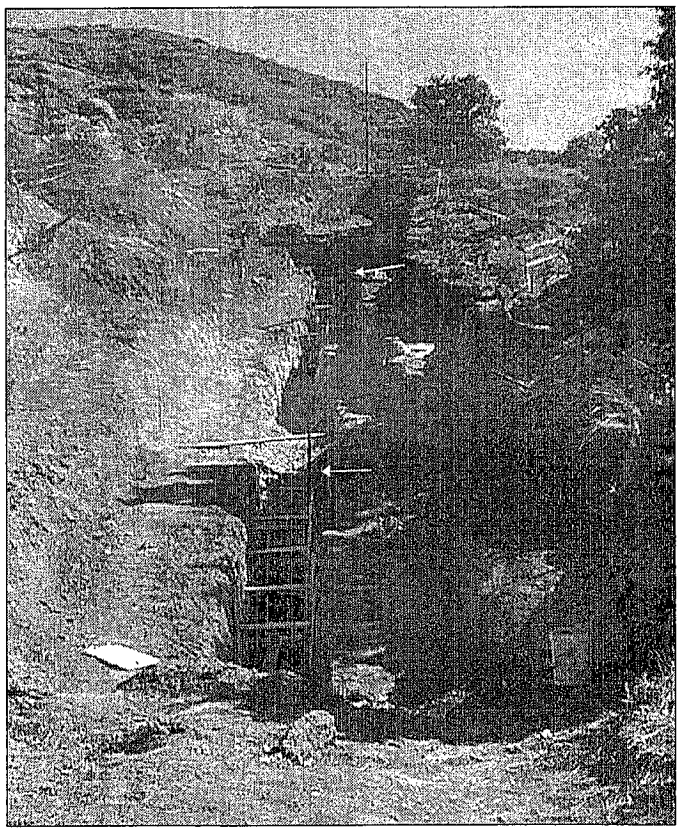

Figure 13. View to the east of the "megatrench" at Little Cottonwood Canyon during the summer of 2000 that exposed 18 m of Holocene and late Pleistocene stratigraphy across two fault scarps. White arrows indicate location of major west-dipping (upper arrow) and east-dipping (lower arrow) fault zones exposed in the trench (McCalpin, 2002). Photo by B. Black.

Trenching at South Fork Dry Creek and Dry Gulch showed that four rather than two surface-faulting earthquakes have occurred on the Salt Lake City segment in the past ~6000 yr (Table 3), thus greatly reducing the mean recurrence time for surface faulting for the segment during the Holocene and substantially raising the segment's hazard potential.

GEO-HAZ Consulting Inc. and the return to Little Cottonwood Canyon. In 2000, GEO-HAZ Consulting, Inc., also with NEHRP funding, reoccupied the Woodward-Clyde site in the Little Cottonwood graben and excavated a single "megatrench" across two fault scarps totaling 18 m high (McCalpin, 2002). The trench and an accompanying auger hole exposed 26 m of vertical section, roughly four times that of a typical trench on the Wasatch fault zone (Fig. 13). Each of the two fault scarps was underlain by a major, down-to-the-west normal fault with 7–9.5 m of vertical displacement measured on Lake Bonneville lacustrine sediments. The trench also exposed two minor antithetic faults; however, they lacked any surface expression, having been buried by wash-facies colluvium shed from the larger scarps. The megatrench was 65 m long but did not extend across the graben and therefore did not expose the large graben-bounding antithetic fault on the west side of Wasatch Boulevard (Fig. 12).

The megatrench contained evidence for seven paleoearthquakes younger than the Bonneville flood at ca. 18 ka and possibly an eighth earthquake that occurred while Lake Bonneville was at or near its highstand at the Bonneville shoreline (Fig. 14). The GEO-HAZ study established the composite surface faulting chronology for the Wasatch fault at Little Cottonwood Canyon shown in Table 4.

McCalpin (2002) states that the age constraints for paleoearthquakes resulting from the megatrench study are not as closely limiting as those resulting from the Black et al. (1996) study at the South Fork Dry Creek and Dry Gulch sites (Table 3). He attributes the discrepancy in part to the fact that organic matter in the megatrench was not always found near paleoearthquake event horizons and that some earthquake ages from the megatrench are based on ^{14}C ages on organics from crack fills rather than from paleosols beneath colluvial wedges.

Utah Quaternary Fault Parameters Working Group. In 2003, the Utah Geological Survey convened the Utah Quaternary Fault Parameters Working Group, a panel of expert paleoseismologists and seismologists, to make a comprehensive evaluation of the paleoseismic-trenching data available for Utah's Quaternary

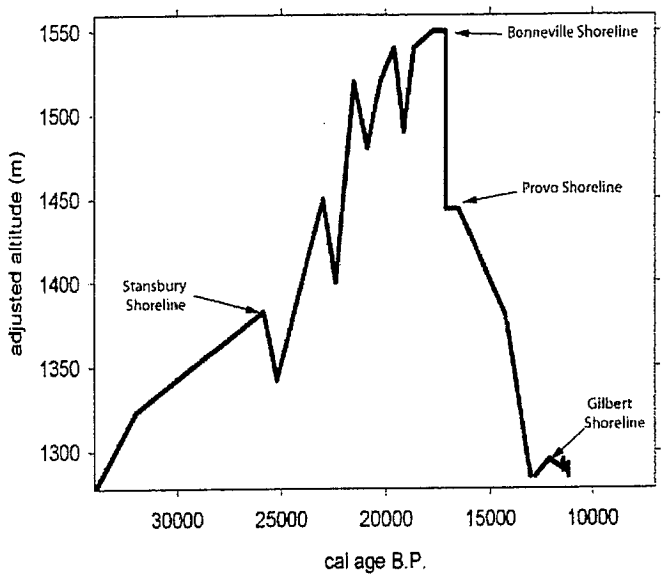

Figure 14. Hydrograph showing the timing of major shorelines of Pleistocene Lake Bonneville (after Oviatt, 1997).

TABLE 4. EARTHQUAKE TIMING DETERMINED FROM THE MEGATRENCH EXCAVATED AT THE LITTLE COTTONWOOD CANYON SITE

Event*	Timing
Z	1.3 ka
Y	2.3 ka
X	3.5 ka
W	5.3 ka
V	7.5 ka
U	9 ka
T	17 ka
S(?)	Possibly between 17 and 20 ka

Note: Earthquake timing based on McCalpin (2002).
*Events Z to W: identification and timing based on colluvial-wedge stratigraphy and radiocarbon ages. Events V to S: identification based on stratigraphic relations in the trench that include the absence or thinning of deposits attributed to erosion following surface faulting and retrodeformation of faulting. The timing of events V and U are constrained by sparse ^{14}C ages; the timing of events T and S are inferred from Lake Bonneville stratigraphy at the trench site.

faults, and where the data permitted, to assign consensus earthquake timing, recurrence interval, and vertical slip-rate estimates for the faults and/or fault sections under review (Lund, 2005). As part of the review, the Working Group considered all of the paleoseismic trenching data available for the Salt Lake City segment.

The Working Group concluded that all reliable paleoearthquake timing, recurrence, size, vertical net displacement, and slip-rate information for the Salt Lake City segment comes from studies either conducted at Little Cottonwood Canyon or at the South Fork Dry Creek and Dry Gulch sites a few km to the south (see above). The Working Group's consensus paleoseismic parameters for the Salt Lake City segment are summarized in Table 5. The Working Group's consensus earthquake timing and recurrence interval and vertical slip-rate estimates represent the best available paleoseismic information for the Salt Lake City segment until superseded by data from future studies.

Summary

The Wasatch fault at Little Cottonwood Canyon has been of great interest to geologists for almost 130 yr. This location played a key role both in the initial understanding of Basin and Range tectonics and later in developing the science of paleoseismology. Investigators conducting multiple paleoseismic studies at and near Little Cottonwood Canyon over the past 26 years have identified four surface faulting earthquakes since the middle Holocene (ca. 6 ka) based on colluvial-wedge stratigraphy, tectonic crack fills, and fault terminations. The timing of these earthquakes is provided by ^{14}C ages on both charcoal and bulk organic samples (primarily paleosol A horizons and tectonic crack-fill deposits). Both the number of earthquakes and their timing are considered well constrained, as is the resulting mean recurrence between surface-faulting earthquakes since the middle Holocene of 1300 ± 400 yr (Lund, 2005).

Three older earthquakes (T, U, V), and a possible fourth oldest earthquake (S) were identified from secondary stratigraphic relations in the Little Cottonwood megatrench and retrodeformation of faulting in the trench. These four earthquakes lack direct stratigraphic or structural evidence (colluvial wedges, crack-fill deposits, fault terminations) of their occurrence (McCalpin, 2002). However, even though the timing of these earthquakes is only broadly constrained, a comprehensive review by the Utah Quaternary Fault Parameters Working Group found the evidence for these earthquakes compelling (Lund, 2005). Available data indicate two recurrence intervals of ~2 k.y. in mid- to early Holocene time, preceded by a >7 k.y. period of surface faulting quiescence.

Evidence from Little Cottonwood Canyon and other nearby sites shows that the elapsed time since the most recent surface faulting on the Salt Lake City segment is equal to or greater than the Working Group's preferred recurrence interval estimate (500–1300–2400 yr) for the segment, indicating that the Salt Lake City segment is a candidate for the next large surface faulting earthquake on the Wasatch fault.

CONCLUSIONS

The Wasatch fault poses a significant seismic hazard to north-central Utah's urban population, based on decades of research that has identified a well-documented chronology of Holocene surface faulting along the fault's six central segments. Study of the Wasatch fault has contributed greatly to the development of the science of paleoseismology and to our

TABLE 5. UTAH QUATERNARY FAULT PARAMETERS WORKING GROUP CONSENSUS PALEOSEISMIC PARAMETERS FOR THE SALT LAKE CITY SEGMENT OF THE WASATCH FAULT

Consensus earthquake timing*	Interevent recurrence†	Weighted mean recurrence three most recent events§	Consensus holocene mean recurrence#	Consensus vertical slip rate**
Z: 1300 ± 650 cal yr B.P.				
	1150 ± 900 cal yr			
Y: 2450 ± 550 cal yr B.P.				
	1500 ± 800 cal yr	1300 ± 400 cal yr		
X: 3950 ± 550 cal yr B.P.				
	1350 ± 900 cal yr		500–**1300**–2400 yr	0.6–**1.2**–4.0 mm/yr
W: 5300 ± 750 cal yr B.P.				
V: ca. 7.5 ka (<8.8–9.1 ka; >5.1–5.3 ka)				
U: ca. 9 ka (≤ 9.5-9.9 ka)				
T: ca. 17 ka				
S(?): 17–20 ka				

Note: From Lund (2005).

*Timing for earthquakes W, X, Y, and Z is from Black et al. (1996). The ± confidence limits have been increased for each earthquake to accommodate the full range of limiting ^{14}C ages used to constrain the timing of the earthquakes; the resulting ± ranges account for both the laboratory and geologic uncertainty associated with the timing of each earthquake (Lund, 2005). McCalpin (2002) identified earthquakes V, U, T, and S at Little Cottonwood Canyon based on stratigraphic relations and a retrodeformation analysis of structural relations in the megatrench. No direct evidence (colluvial wedges, tectonic crack fills, fault terminations) was found to document these earthquakes, and consequently their timing is only broadly constrained.

†The ± confidence limits equal the square root of the sum of the squares of the individual ± confidence limits for each bracketing earthquake rounded to nearest 100 yr.

§Weighted mean rounded to nearest 100 yr; 2-sigma confidence limits rounded to nearest 100 yr. The weighted mean recurrence for the three most recent surface-faulting earthquakes on the Salt Lake City Segment (SLCS) is ≤ to the elapsed time since the most recent surface-faulting earthquake on the SLCS.

#The Working Group's preferred recurrence-interval and confidence-limit estimates (bold) for the SLCS are based on currently available information on earthquake timing and variability for the SLCS (Lund, 2005).

**The Working Group's preferred vertical slip-rate and confidence-limit estimates (bold) for the SLCS are based on currently available information on earthquake timing and displacement (Lund, 2005).

understanding of Basin and Range Province fault mechanics and tectonic geomorphology. In traversing the Wasatch fault from Nephi to Salt Lake City, we have highlighted evidence for earthquake generation in the subsurface based on the structure and rheology of fault-zone rocks, and identified the timing, displacement, and extent of Holocene and late Pleistocene surface faulting along the fault's central segments. Collectively, the field-trip stops have allowed us to peer into the Wasatch fault's "earthquake engine" and to consider the natural complexity of its pulse.

Along the fault, vertically displaced alluvial, glacial, and lacustrine deposits demonstrate a long history of Quaternary normal faulting; however, geomorphic relations and paleoseismic trench studies on the central Wasatch fault segments suggest higher rates of faulting during the Holocene than during the late Pleistocene. Additional paleoseismic studies along the Wasatch fault are necessary to test possible slip-rate variations and segmentation along the fault, and to refine the timing, recurrence, and coseismic displacement of surface faulting earthquakes. Important unresolved issues remain, including determining the fault's subsurface geometry and potential for aseismic creep and resolving discrepancies between geologic slip rates and geodetic extension rates. Evaluating these issues is critical to characterize future surface faulting earthquakes on the Wasatch fault and the earthquake hazard along the Wasatch Front.

ACKNOWLEDGMENTS

We thank Joel Pederson (Utah State University), and Gary Christenson and Michael Hylland (Utah Geological Survey) for carefully reviewing this field trip guide. Research on the Nephi segment (Stop 1) was supported by National Science Foundation grant EAR-0207373; fault trenching at the Santaquin site (Stop 2) was supported by the Utah Geological Survey and the U.S. Geological Survey National Earthquake Hazards Reduction Program, and land access was granted by the U.S. Forest Service.

REFERENCES CITED

Andrews, D.J., and Bucknam, R.C., 1987, Fitting degradation of shoreline scarps by a nonlinear diffusion model: Journal of Geophysical Research, v. 92, no. B12, p. 12,857–12,867.

Arabasz, W.J., and Julander, D.R., 1986, Geometry of seismically active faults and crustal deformation within the Basin and Range—Colorado Plateau transition, *in* Mayer, L., ed., Extensional tectonics of the southwestern United States: A perspective on processes and kinematics: Geological Society of America Special Paper 208, p. 43–74.

Arabasz, W.J., Smith, R.B., and Richins, W.D., 1979, Earthquake studies along the Wasatch Front, Utah: Network monitoring, seismicity and seismic hazards, *in* Arabasz, W.J., Smith, R.B., and Richins, W.D., eds., Earthquake studies in Utah, 1850–1978: Salt Lake City, University of Utah Seismograph Stations, p. 253–285.

Arabasz, W.J., Pechmann, J.C., and Brown, E.D., 1992, Observational seismology and the evaluations of earthquake hazards and risk in the Wasatch Front area, *in* Gori, P.L., and Hays, W.W., eds., Assessment of regional earthquake hazards and risk along the Wasatch Front, Utah: U.S. Geological Survey Professional Paper 1500-D, 36 p.

Armstrong, P.A., Ehlers, T.A., Chapman, D.S., Farley, K.A., and Kamp, P.J.J., 2003, Exhumation of the central Wasatch Mountains, 1: Pattern and timing deduced from low-temperature thermochronology data: Journal of Geophysical Research, v. 108, no. B3, p. 2172, doi: 10.1029/2001JB001708.

Armstrong, P.A., Taylor, A.R., and Ehlers, T.A., 2004, Is the Wasatch fault (Utah, United States) footwall segmented over million-year time scales?: Geology, v. 32, p. 385–388, doi: 10.1130/G20421.1.

Black, B.D., Lund, W.R., Schwartz, D.P., Gill, H.E., and Mayes, B.H., 1996, Paleoseismic investigation on the Salt Lake City segment of the Wasatch fault zone at the South Fork Dry Creek and Dry Gulch sites, Salt Lake County, Utah: Utah Geological Survey Special Study 92, 22 p.

Black, B.D., Hecker, S., Hylland, M.D., Christenson, G.E., and McDonald, G.N., 2003, Quaternary fault and fold database and map of Utah: Utah Geological Survey Map 193DM, scale 1:500,000, CD-ROM.

Bruhn, R.L., Yonkee, W.A., and Parry, W.T., 1990, Structural and fluid-chemical properties of seismogenic normal faults: Tectonophysics, v. 175, p. 139–157, doi: 10.1016/0040-1951(90)90135-U.

Bruhn, R.L., Gibler, P.R., Houghton, W., and Parry, W.T., 1992, Structure of the Salt Lake segment, Wasatch normal fault zone: Implications for rupture propagation during normal faulting, *in* Gori, P.L., and Hays, W.W., eds., Assessment of regional earthquake hazards and risk along the Wasatch Front, Utah: U.S. Geological Survey Professional Paper 1500-C, 16 p.

Bruhn, R.L., Parry, W.T., Yonkee, W.A., and Thompson, T., 1994, Fracturing and hydrothermal alteration in normal fault zones: Pure and Applied Geophysics, v. 142, p. 609–643, doi: 10.1007/BF00876057.

Bryant, B., Naeser, C.W., Marvin, R.F., and Mehnert, H.H., 1989, Ages of late Paleogene and Neogene tuffs and the beginning of rapid regional extension, eastern boundary of the Basin and Range Province near Salt Lake City, Utah: U.S. Geological Survey Bulletin 1787, 37 p.

Bucknam, R.C., 1978, Northwestern Utah seismotectonics studies, *in* Seiders, W., and Thomson, J., compilers, Summaries of technical reports, v. VII: Menlo Park, California, U.S. Geological Survey Office of Earthquake Studies, p. 64.

Chang, W.L., 1998, Earthquake hazards on the Wasatch fault—tectonically induced flooding and stress triggering of earthquakes [M.S. thesis]: Salt Lake City, University of Utah, 123 p.

Chang, W.L., and Smith, R.B., 2002, Integrated seismic-hazard analysis of the Wasatch Front, Utah: Bulletin of the Seismological Society of America, v. 92, no. 5, p. 1904–1922, doi: 10.1785/0120010181.

DuRoss, C.B., 2004, Spatial and temporal trends of surface rupturing on the Nephi segment of the Wasatch fault, Utah—implications for fault segmentation and the recurrence of paleoearthquakes [M.S. thesis]: Salt Lake City, University of Utah, 120 p.

DuRoss, C.B., and Bruhn, R.L., 2005, Active tectonics of the Nephi segment, Wasatch fault zone, Utah, *in* Lund, W.R., ed., Western States Seismic Policy Council Proceedings Volume of the Basin and Range Province Seismic Hazards Summit II: Utah Geological Survey Miscellaneous Publication 05-2, CD-ROM.

Emmons, B.F., 1878, U.S. Geological Expedition 40th Parallel Report, v. 2, 357 p.

Evans, J.P., Yonkee, W.A., Parry, W.T., and Bruhn, R.L., 1997, Fault-related rocks of the Wasatch normal fault: Brigham Young University Geology Studies, v. 42, Part II, p. 279–297.

Evans, S.H., Parry, W.T., and Bruhn, R.L., 1985, Thermal, mechanical and chemical history of Wasatch fault cataclasite and phyllonite, Traverse Mountains area, Salt Lake City, Utah: From K/Ar and fission track measurements: U.S. Geological Survey Open-File Report 86-31, p. 410–415.

Friedrich, A.M., Wernicke, B.P., Niemi, N.A., Bennett, R.A., and Davis, J.L., 2003, Comparison of geodetic and geologic data from the Wasatch region, Utah, and implications for the spectral character of Earth deformation at periods of 10 to 10 million years: Journal of Geophysical Research, v. 108, no. B4, 2199, doi: 10.1029/2001JB000682.

Gilbert, G.K., 1872, Reports on exploration in Nevada and Arizona [abs.]: Forty-second Congress, second session, Senate Document 65, p. 90–94.

Gilbert, G.K., 1875, Report on the geology of portions of Nevada, Utah, California, and Arizona examined in the years 1871 and 1872: Report on U.S. Geographical and Geological Surveys west of the 100th meridian, v. 3, Geology: Pt. 1, p. 17–187.

Gilbert, G.K., 1884, A theory of the earthquakes of the Great Basin, with a practical application: American Journal of Science, Third Series, v. XXXVII, no. 157, Article XI, p. 49–53.

Gilbert, G.K., 1890, Lake Bonneville: U.S. Geological Survey Monograph 1, 438 p.

Gilbert, G.K., 1928, Studies of Basin and Range structure: U.S. Geological Survey Professional Paper 153, 89 p.

Hanson, K.L., Swan, F.H., and Schwartz, D.P., 1981, Study of earthquake recurrence intervals on the Wasatch fault, Utah: San Francisco, California, Woodward-Clyde Consultants, Sixth-annual technical report prepared for U.S. Geological Survey under contract no. 14-08-0001-19115, 22 p.

Harris, R.A., Smith, R.B., Chang, W.L., Meertens, C., and Friedrich, A., 2000, Temporal distribution of extensional strain across the southern Wasatch fault zone—geological constraints for the GPS velocity field: Eos (Transactions, American Geophysical Union), v. 81, p. 1230.

Harty, K.M., Mulvey, W.E., and Machette, M.N., 1997, Surficial geologic map of the Nephi segment of the Wasatch fault zone, eastern Juab County, Utah: Utah Geological Survey Map 170, 14 p., 1 pl., scale 1:50,000.

Hintze, 1988, Geologic history of Utah: Provo, Brigham Young University, 202 p.

Hunt, C.B., ed., 1982, Pleistocene Lake Bonneville, ancestral Great Salt Lake, as described in notebooks of G.K. Gilbert, 1875–1880: Brigham Young Geology Studies, v. 29, part 1, 231 p.

Hylland, M.D., and Machette, M.N., 2004, Interim surficial geologic map of the Levan segment of the Wasatch fault zone, Juab and Sanpete Counties, Utah, *in* Christenson, G.E., Ashland, F.X., Hylland, M.D., McDonald, G.N., and Case, B., Database compilation, coordination of earthquake-hazards mapping, and study of the Wasatch fault and earthquake-induced landslides, Wasatch Front, Utah: U.S. Geological Survey, National Earthquake Hazards Reduction Program Final Technical Report, award no. 03HQAG0008, variously paginated, scale 1:50,000.

Jackson, M., 1991, Number and timing of Holocene paleoseismic events on the Nephi and Levan segments, Wasatch fault zone, Utah: Utah Geological Survey Special Study 78, 23 p.

King, C., 1878, U.S. Geological Expedition 40th Parallel Report, v. 1, p. 745–746.

Kowallis, B.J., Ferguson, J., and Jorgensen, G.J., 1990, Uplift along the Salt Lake segment of the Wasatch fault from apatite and zircon dating in the Little Cottonwood stock, *in* Durani, S.A., and Benton, E.V., eds., Proceedings of the 6th International Fission Track Dating Workshop, Nuclear Tracks and Radiation Measurements 17: Oxford, Pergamon, p. 325–329.

Lee, J.-J., and Bruhn, R.L., 1996, Characterization of the structural anisotropy of normal fault surfaces: Journal of Structural Geology, v. 18, p. 1043–1059, doi: 10.1016/0191-8141(96)00022-3.

Lund, W.R., 2005, Consensus preferred recurrence-interval and vertical slip-rate estimates—Review of Utah paleoseismic-trenching data by the Utah Quaternary Fault Parameters Working Group: Utah Geological Survey Bulletin 130, CD-ROM.

Lund, W.R., and Black, B.D., 1998, Paleoseismic investigation at Rock Canyon, Provo segment, Wasatch fault zone, Utah County, Utah: Special Study #93, Utah Geological Survey, 21 p.

Lund, W.R., Schwartz, D.P., Mulvey, W.E., Budding, K.E., and Black, B.D., 1991, Fault behavior and earthquake recurrence of the Provo segment of the Wasatch fault zone at Mapleton, Utah County, Utah: Utah Geological and Mineral Survey Special Studies 75, 41 p.

Mabey, D.R., 1992, Subsurface geology along the Wasatch fault area, Utah, *in* Gori, P.L., and Hays, W.W., eds., Assessment of regional earthquake hazards and risk along the Wasatch Front, Utah: U.S. Geological Survey Professional Paper 1500-C, 16 p.

Machette, M.N., 1992, Surficial geologic map of the Wasatch fault zone, eastern part of Utah Valley, Utah County and parts of Salt Lake and Juab Counties, Utah: U.S. Geological Survey Miscellaneous Investigations Series Map I-2095, scale 1:50,000, pamphlet 30 p.

Machette, M.N., Personius, S.F., and Nelson, A.R., 1992, Paleoseismology of the Wasatch fault zone—A summary of recent investigations, interpretations, and conclusions, *in* Gori, P.L., and Hays, W.W., eds., Assessment of regional earthquake hazards and risk along the Wasatch Front, Utah: U.S. Geological Survey Professional Paper 1500-A, p. A1–A71.

Martinez, L.J., Meertens, C.M., and Smith, R.B., 1998, Rapid deformation rates along the Wasatch fault zone, Utah, from first GPS measurements with implications for earthquake hazard: Geophysical Research Letters, v. 25, no. 4, p. 567–570, doi: 10.1029/98GL00090.

Mattson, A., and Bruhn, R.L., 2001, Fault slip rates and initiation age based on diffusion equation modeling—Wasatch fault zone and eastern Great Basin: Journal of Geophysical Research, v. 106, no. B7, p. 13,739–13,750, doi: 10.1029/2001JB900003.

McCalpin, J.P., editor, 1996, Paleoseismology: San Diego, Academic Press, 588 p.

McCalpin, J.P., 2002, Post-Bonneville paleoearthquake chronology of the Salt Lake City segment, Wasatch fault zone, from the 1999 "Megatrench" site: Utah Geological Survey Miscellaneous Publication 02-7, 37 p.

McCalpin, J.P., and Nishenko, S.P., 1996, Holocene paleoseismicity, temporal clustering, and probabilities of future large (M >7) earthquakes on the Wasatch fault zone, Utah: Journal of Geophysical Research, v. 101, no. B3, p. 6233–6253, doi: 10.1029/95JB02851.

Oviatt, C.G., 1997, Lake Bonneville fluctuations and global climate change: Geology, v. 25, p. 155–158, doi: 10.1130/0091-7613(1997)025<0155:LBFAGC>2.3.CO;2.

Pack, F.J., 1926, New discoveries relating to the Wasatch fault: American Journal of Science, v. 27, p. 399–410.

Parry, W.T., and Bruhn, R.L., 1986, Pore fluid and seismogenic characteristics of fault rock at depth on the Wasatch fault, Utah: Journal of Geophysical Research, v. 91, p. 730–744.

Parry, W.T., and Bruhn, R.L., 1987, Fluid inclusion evidence for minimum 11 km vertical offset on the Wasatch normal fault, Utah: Geology, v. 15, p. 67–70, doi: 10.1130/0091-7613(1987)15<67:FIEFMK>2.0.CO;2.

Parry, W.T., Wilson, P.N., and Bruhn, R.L., 1988, Pore fluid chemistry and chemical reactions on the Wasatch normal fault, Utah: Geochimica et Cosmochimica Acta, v. 52, p. 2053–2063, doi: 10.1016/0016-7037(88)90184-6.

Personius, S.F., and Scott, W.E., 1992, Surficial geology of the Salt Lake City segment and parts of adjacent segments of the Wasatch fault zone, Davis, Salt Lake, and Utah Counties, Utah: U.S. Geological Survey Miscellaneous Investigation Series Map I-2106, scale 1:50,000.

Schwartz, D.P., and Coppersmith, K.J., 1984, Fault behavior and characteristic earthquakes—Examples from the Wasatch and San Andreas fault zones: Journal of Geophysical Research, v. 89, no. B7, p. 5681–5698.

Schwartz, D.P., and Lund, W.R., 1988, Paleoseismicity and earthquake recurrence at Little Cottonwood Canyon, Wasatch fault zone, Utah, *in* Machette, M.N., ed., In the footsteps of G.K. Gilbert—Lake Bonneville and neotectonics of the eastern Basin and Range Province, Guidebook for Field Trip Twelve: Utah Geological and Mineral Survey Miscellaneous Publication 88-1, p. 82–85.

Smith, R.B., and Bruhn, R.L., 1984, Intraplate extensional tectonics of the eastern Basin-Range: Inferences on structural style from seismic reflection data, regional geophysics and thermal mechanical models of brittle-ductile deformation: Journal of Geophysical Research, v. 87, p. 5733–5762.

Swan, F.H., III, Schwartz, D.P., and Cluff, L.S., 1980, Recurrence of moderate to large magnitude earthquakes produced by surface faulting on the Wasatch fault zone, Utah: Bulletin of the Seismological Society of America, v. 70, p. 1431–1462.

Swan, F.H., III, Hanson, K.L., Schwartz, D.P., and Knuepfer, P.L., 1981, Study of earthquake recurrence intervals on the Wasatch fault, Utah—Little Cottonwood Canyon site: U.S. Geological Survey Open-File Report 81-450, 30 p.

Wallace, R.E., 1980, G.K. Gilbert's studies of faults, scarps, and earthquakes, *in* Yochelson, E.L., ed., The scientific ideas of G.K. Gilbert; An assessment on the occasion of the centennial of the United States Geological Survey (1879–1979): Geological Society of America Special Paper 183, p. 35–44.

Wheeler, R.L., and Krystinik, K.B., 1992, Persistent and nonpersistent segmentation of the Wasatch fault zone, Utah–statistical analysis for evaluation of seismic hazard, *in* Gori, P.L., and Hays, W.W., eds., Assessment of regional earthquake hazards and risk along the Wasatch Front, Utah: U.S. Geological Survey Professional Paper 1500-B, p. B-1–B-47.

Yonkee, W.A., and Bruhn, R.L., 1990, Geometry and mechanics of a structural boundary, Wasatch fault zone, Utah, *in* Bruhn, R.L., Lee, J-J, and Yonkee, W.A., eds., Structural properties of the American Fork, Provo, and Spanish Fork subsegments, Wasatch normal fault zone, Utah: Utah Geological and Mineral Survey Open-File Report 186, 50 p.

Zoback, M.L., 1983, Structure and Cenozoic tectonism along the Wasatch fault zone, Utah, *in* Miller, D.M., Todd, V.R., and Howard, K.A., eds., Tectonic and stratigraphic studies in the eastern Great Basin: Geological Society of America Memoir 157, p. 3–27.

Printed in the USA